Journal of Medicinal Chemistry

Article

Design, Synthesis and Antifibrosis Activity in Liver of Nonsecosteroidal Vitamin D Receptor Agonists with Phenyl-pyrrolyl Pentane Skeleton

Cong Wang, Bin Wang, Lingjing Xue, Zisheng Kang, Siyuan Hou, Junjie Du, and Can Zhang

J. Med. Chem., **Just Accepted Manuscript** • DOI: 10.1021/acs.jmedchem.8b01165 • Publication Date (Web): 10 Oct 2018

Design, Synthesis and Antifibrosis Activity in Liver of Nonsecosteroidal Vitamin D Receptor Agonists with Phenyl-pyrrolyl Pentane Skeleton

Cong Wang [a,b1], Bin Wang[a,1], Lingjing Xue[a], Zisheng Kang[a], Siyuan Hou[a], Junjie Du[a], Can Zhang[a,*]

[a]State Key Laboratory of Natural Medicines and Jiangsu Key Laboratory of Drug Discovery for Metabolic Diseases, Center of New Drug Discovery, China Pharmaceutical University, 24 Tong Jia Xiang, Nanjing, 210009, China.

[b]Fujian Provincial Key Laboratory of Hepatic Drug Research

***Correspondence should be addressed to:**

Tel/Fax: 86-25-83271171; E-mail: zhangcan@cpu.edu.cn

ABSTRACT: Liver fibrosis is characterized by excessive deposition of extracellular matrix (ECM) components and results to impairment of liver function. Vitamin D plays a critical role in the development of liver fibrosis as it inhibits transforming growth factor β1 (TGFβ1)-induced excessive deposition of ECM in activated hepatic stellate cells (HSCs). Here, a series of novel nonsecosteroidal Vitamin D receptor (VDR) agonists with phenyl-pyrrolyl pentane skeleton was designed and synthesized. Among them, seven compounds including **15a** exhibited more efficient inhibitory activity in collagen deposition and fibrotic gene expression. Histological examination results displayed that compound **15a** treatment prevented the development of hepatic fibrosis that induced by carbon tetrachloride (CCl_4) injections in mice. In addition, compound **15a**, unlike the positive control calcipotriol and $1,25(OH)_2D_3$, did not cause hypercalcemia that is toxic to nerve, heart and many other organs. These findings provide novel insights into drug discoveries for hepatic fibrosis using nonsecosteroidal VDR modulators.

INTRODUCTION

Liver fibrosis, characterized by excessive accumulation of extracellular matrix (ECM) and loss of pliability and liver function, is the result of wound-healing responses that triggered by either chronic or acute liver injury,[1-3] such as alcohol abuse, chronic hepatitis virus (hepatitis B virus/hepatitis C virus) infection, and increasingly, nonalcoholic steatohepatitis (NASH), nonalcoholic fatty liver disease (NAFLD).[4-6] With continuous injury, the fibrillar collagens were progressively deposited and parenchymal nodules were surrounded by collagen bands, eventually leading to the histological signature of hepatic cirrhosis which represents a major global health concern. At present, the only way to treat the end-stage cirrhosis is liver transplantation.[7] However, the condition of the potential recipients, especially the number of available donor organs, limited the applicability of this technique even in the developed world.[8] Moreover, the Food and Drug Administration has not yet approved anti-fibrotic therapies for chronic liver disease.[9]

Hepatic stellate cells (HSCs) are established as a major cellular source of ECM and the main driver of liver fibrogenesis. In healthy liver cells, HSCs remains quiescent and the main function is storing vitamin A.[10] Once being activated following liver injury, HSCs would entered into a α-smooth muscle actin (α-SMA) positive phenotypic transformation and differentiate into ECM-secreting cells. The activated HSCs produce a considerable amount of collagen I, which is the main components of ECM, resulting in the loss of liver pliability and function.[11]

Transforming growth factor β1 (TGFβ1) is one of the most potent pro-fibrotic modulators. In paracrine and autocrine fashion, TGFβ1 promotes HSCs activation and contributes to fibrotic processes in liver.[12, 13] Therefore, the inhibition of TGFβ1 pathway to reduce ECM production in HSCs is recognized as an effective anti-fibrotic strategy. While the precise mechanisms of regulating ECM synthesis via TGFβ1 pathway have yet to be elucidated, vitamin D has been established in close relationship with TGFβ1 and liver fibrosis development. Previous studies demonstrated a beneficial effect for 1,25$(OH)_2D_3$ (**1**, Figure 1), the most active form of vitamin D, to attenuate liver fibrosis.[14-16]

It is widely recognized that 1,25$(OH)_2D_3$ plays a pivotal role in the homeostasis of calcium and phosphorus, cell proliferation and differentiation, as well as immunomodulation.[17, 18] 1,25$(OH)_2D_3$ exerts actions through promoting gene transcription by binding to vitamin D receptor (VDR), which belonging to the superfamily of nuclear receptor. VDR is robust expressed in HSCs and fully functional in these cells.[19] In 2013, Ding et al. reported that calcipotriol, an analog of 1,25$(OH)_2D_3$, could inhibit the collagen I and α-SMA expression via reducing the occupancy of SMAD3 at these sites and antagonizing a wide range of transcriptional responses on profibrotic genes that dependent on TGFβ/SMAD signaling pathway.[20] These findings suggest that VDR is an checkpoint to modulate the liver wound-healing response and VDR ligands may as a potential therapy for the treatment of liver fibrosis.

VDR ligands have already been attractive therapeutics against psoriasis, osteoporosis, and cancer.[21-23] At present, more than 3000 VDR modulators with secosteroid skeleton have been synthesized and biologically evaluated as drug candidates,[24] such as calcipotriol (**2**) and paricalcitriol (**3**). Almost all of the VDR ligands with high activity have the same secosteroidal skeleton as **1**-**3**, structurally, consisting of the A-ring that borne two hydroxyl groups, a triene moiety or conjugated diene, a side chain, and the CD-ring. Although many compounds exhibit efficient VDR activity in *in vitro* and *in vivo* studies, their synthetic inconvenience, structural complexity, chemical instability, as well as hypercalcemia limit the clinical application in the treatment of liver fibrosis. Recently, a lot of attention has been drawn to nonsecosteroidal vitamin D mimics,[25-28] such as bisphenol derivative (**4**),[29] tris-aromatic derivatives (**5**),[21] carborane derivatives (**6**),[30-33] due to their less calcium mobilization and simpler structures. Previously, we have reported phenyl-pyrrolyl pentane skeleton as a novel nonsecosteroidal VDR ligand skeleton which possessed the potential to inhibit proliferation of cancer cells without inducing hypercalcemia effect.[34-36] However, we found some compounds had no effect on cancer cells but show significantly inhibitory effect on HSCs activation, indicating that VDR agonists may affect HSCs more strongly than cancer cells. Therefore, it is noteworthy to verify whether these nonsecosteroidal vitamin D ligands can act as effective as $1,25(OH)_2D_3$ or calcipotriol that with secosteroidal skeleton for preventing the progression of liver fibrosis but have smaller side effects like hypercalcemia.

To explore the relationship between structure and anti-fibrotic activity for these nonsecosteroidal compounds based on the phenyl-pyrrolyl pentane skeleton, twenty-two new compounds have been designed, synthesized, and examined with various biological assays. Seven compounds showed much better properties than positive control calcipotriol in the anti-collagen I synthetic activities assay. Among them, compound **15a** exhibited more potent inhibitory activity against both fibrotic gene expression and collagen deposition by Q-PCR and western blot assays. Results of histological examination displayed that the treatment of compound **15a** prevented hepatic fibrosis induced by carbon tetrachloride (CCl_4) injection in mice. Moreover, compound **15a** had no significant change on serum calcium that can be raised by positive control calcipotriol or $1,25(OH)_2D_3$.

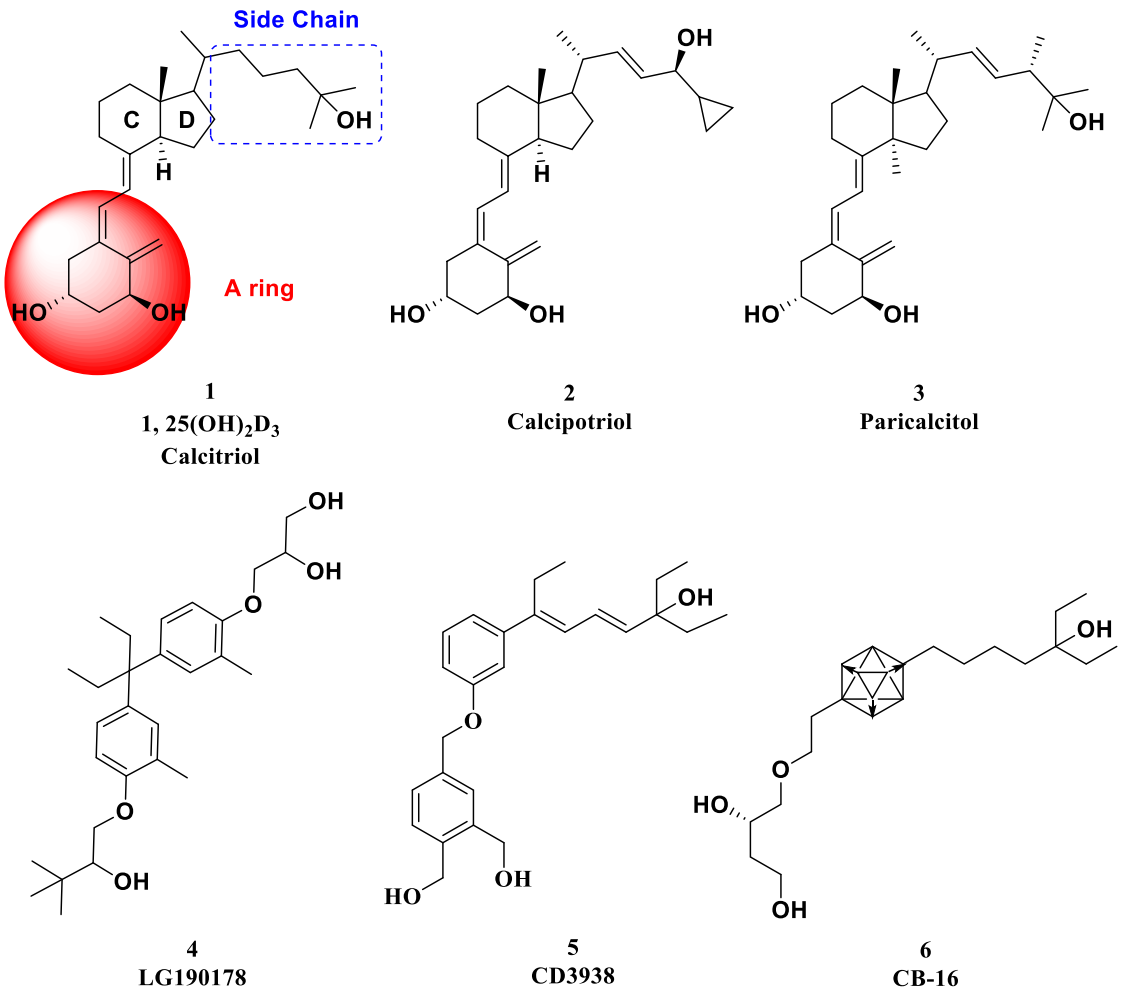

Figure 1. Chemical structures of representative secosteroidal and nonsecosteroidal VDR ligands.

RESULTS AND DISCUSSION

Design of target compounds.

Boehm et al. reported the first nonsecosteroidal analogs of vitamin D_3, LG190178 (**4**) and found that propane-1.2-diol of **4** are important for the binding affinity. Based on the

phenyl-pyrrolyl pentane skeleton and the structure feature of **4**, we designed derivatives **13** using a scaffold hopping strategy and introducing different R_1 substituents to identify anti-fibrotic VDR ligands. Then, phenyl-pentane group on pyrrole ring C-4 position instead of the C-5 position was designed to investigate the influence of the substitution positions of the pyrrole ring, and we obtained compounds **15**. Finally, we further investigated the A ring part of target compounds and designed compounds **17**, **19**, and **20** by substitution of the A ring with other hydrophilic groups, such as the butanoic acid, pentanoic acid, alanine, β-alanine, and succinic acid.

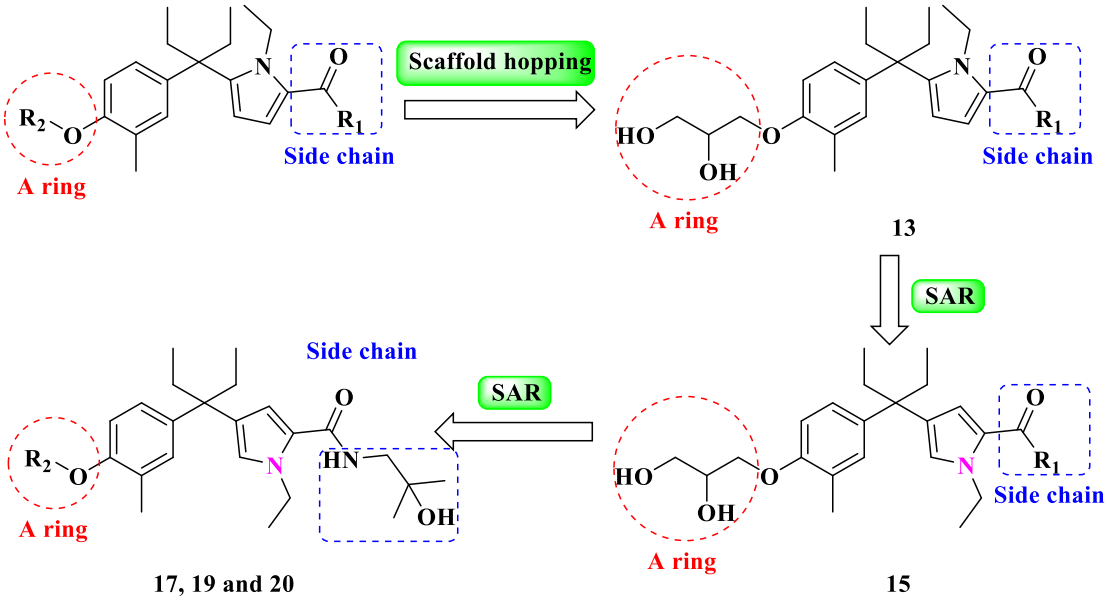

Figure 2. Design of the novel nonsecosteroidal VDR ligands.

Synthetic procedures of target compounds.

The synthetic pathway of target compounds **13a-h** is outlined in Scheme 1. The intermediate **7** was prepared using previously reported approach,[34] then it reacted with

ethyl pyrrole-2-carboxylate at 0°C in the presence of lewis acid $BF_3 \cdot Et_2O$ to produce intermediate **8a**. After the management with iodoethane in DMF, intermediate **9a** was obtained. The reduction reaction of **9a** give the intermediate **10a**, which was hydrolyzed by KOH to produce **11a** in high yield. By reaction with the corresponding amines, **11a** gave intermediates **12a-i**, respectively. Finally, target compounds **13a-h** were obtained by electrophilic substitution of glycidol with intermediates **12a-h** in the presence of NaH.

The synthetic pathway of compounds **15a-i** is outlined in Scheme 2. Intermediate **8b**, the regioselectivity isomer of **8a**, was obtained by reacting with ethyl pyrrole-2-carboxylate at 20°C, instead of at 0°C, in the presence of lewis acid $BF_3 \cdot Et_2O$ in moderate yield. By the same method as described in the synthesis of **9a-13**, target compounds **15a-i** were obtained.

The synthetic pathway of compounds **17a-b**, **19a-b**, and **20** is outlined in Scheme 3. Intermediate **14a** was subjected to nucleophilic substitution with the corresponding halohydrocarbon to give intermediates **16a-b**, which were further treated by hydrolysis of ester groups to afford target compounds **17a-b** in high yield. On the other hand, intermediates **18a-b** were synthesized by treatment of intermediate **14a** with corresponding amino acids. Deprotection of **18a-b** using CF_3COOH yielded target compounds **19a-b**. Compound **20** was obtained by the same method as described in the synthesis of intermediates **16a-b**.

Scheme 1. Synthesis of compounds **13a-h**[a]

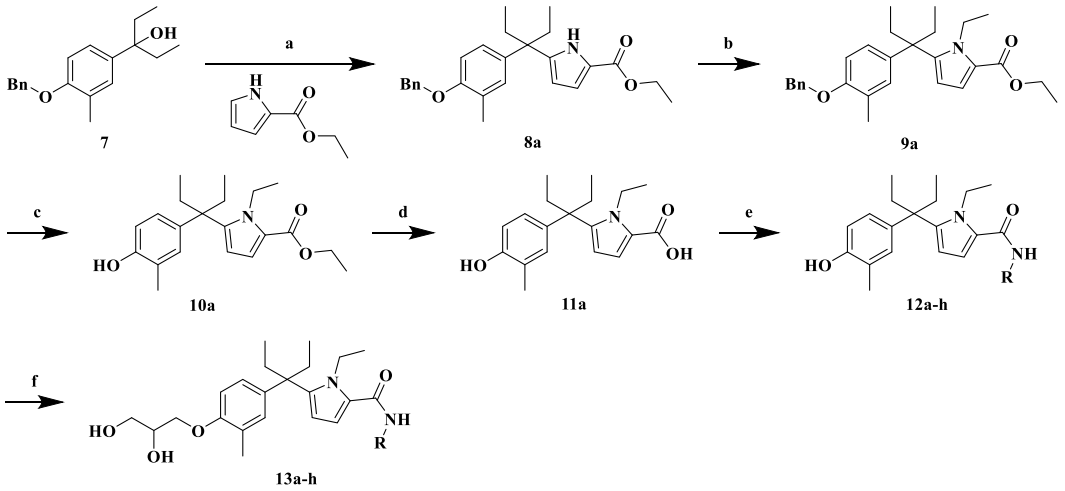

[a]Reagents and conditions: (a) Ethyl 1H-pyrrole-2-carboxylate, $BF_3 \cdot Et_2O$, 0°C, 1 h, 73%; (b) C_2H_5I, NaH, DMF, 0-25°C, 2 h, 82.4%; (c) Pd/C, $HCOONH_4$, CH_3OH/EtOAc (10:1), 25°C, 1 h, 98%; (d) 2 mol/L KOH, EtOH, rt, 1 h, 94%; (e) EDCI, HOBt, TEA, RNH_2, DCM, rt, overnight, 35-96%; (f) Glycidol, NaH, DMF, 80°C, 5 h, 54-82%.

Scheme 2. Synthesis of compounds **15a-i**[a]

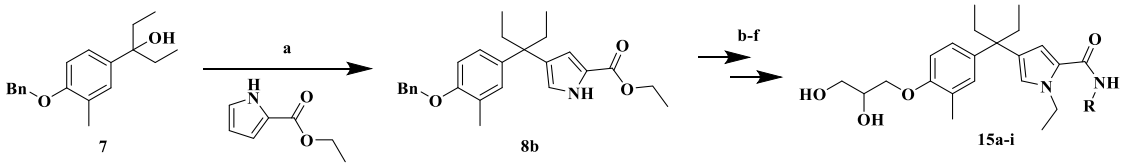

[a]Reagents and conditions: (a) Ethyl 1H-pyrrole-2-carboxylate, $BF_3 \cdot Et_2O$, 25°C, 1 h, 44%; (b) C_2H_5I, NaH, DMF, 0-25°C, 2 h, 85%; (c) Pd/C, $HCOONH_4$, CH_3OH/EtOAc (10:1), 25°C, 1 h, 97%; (d) 2 mol/L KOH, EtOH, rt, 1 h, 95%; (e) EDCI, HOBt, TEA, RNH_2, DCM, rt, overnight, 32-89%; (f) Glycidol, NaH, DMF, 80°C, 5 h, 47-78%.

Scheme 3. Synthesis of compounds **17a-b**, **19a-b**, and **20**[a]

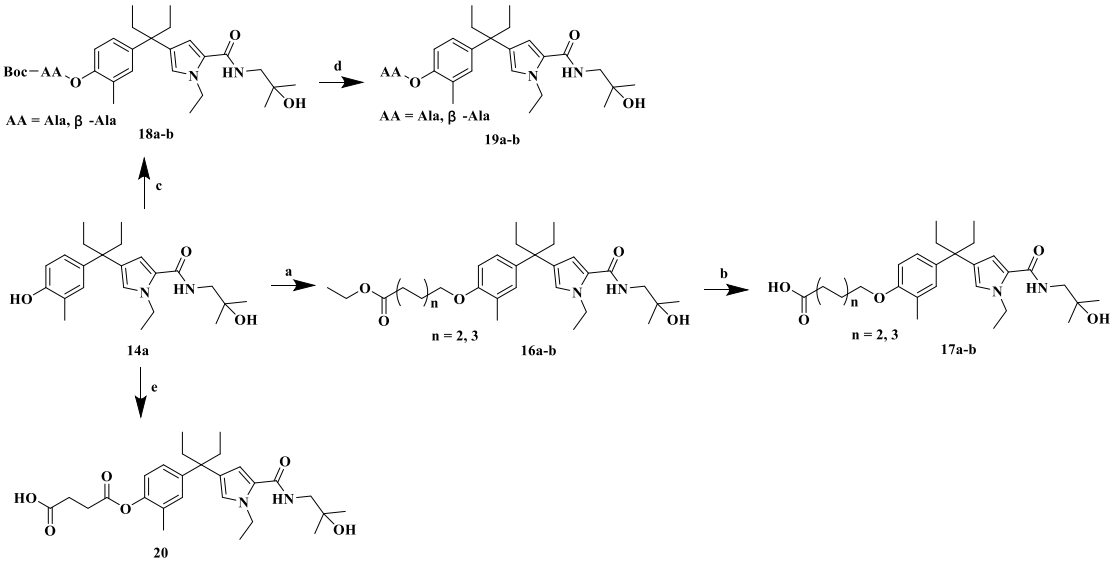

[a]Reagents and conditions: (a) Ethyl 4-bromobutyrate or ethyl 5-bromopentyrate, NaH, DMF, 80°C, 5 h, 58-67%; (b) 2 mol/L KOH, EtOH, rt, 1 h, 95-97%; (c) Boc-AA, EDCI, DMAP, DCM, rt, overnight, 43-52%; (d) TFA, DCM, rt, 1 h, 87-92%; (e) Succinic anhydride, NaH, DMF, 80°C, 2 h, 43%.

Table 1. The structures of all compounds.

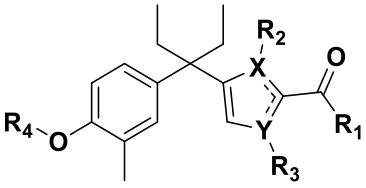

Compd	X	Y	R_1	R_2	R_3	R_4
13a	N	C	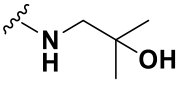	C_2H_5	H	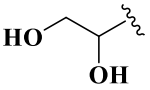

13b	N	C	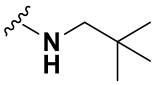	C_2H_5	H	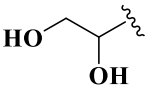
13c	N	C	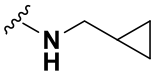	C_2H_5	H	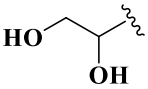
13d	N	C	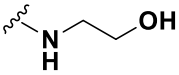	C_2H_5	H	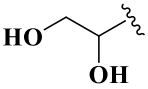
13e	N	C	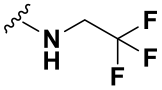	C_2H_5	H	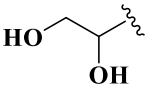
13f	N	C	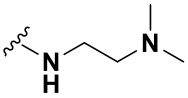	C_2H_5	H	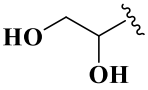
13g	N	C	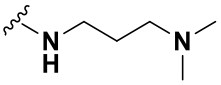	C_2H_5	H	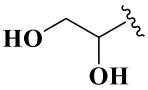
13h	N	C	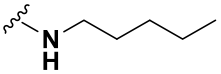	C_2H_5	H	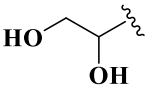
15a	C	N	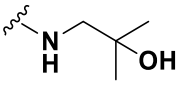	H	C_2H_5	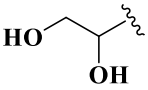
15b	C	N	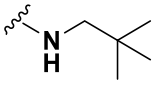	H	C_2H_5	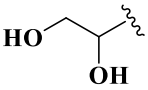
15c	C	N	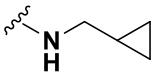	H	C_2H_5	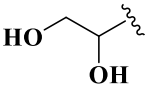

15d	C	N	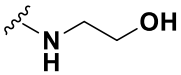	H	C_2H_5	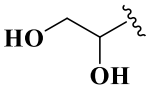
15e	C	N	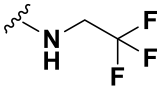	H	C_2H_5	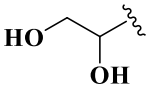
15f	C	N	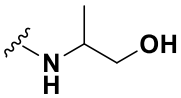	H	C_2H_5	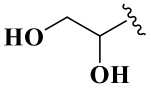
15g	C	N	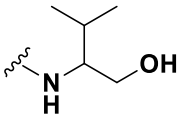	H	C_2H_5	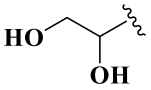
15h	C	N	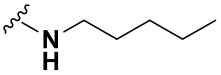	H	C_2H_5	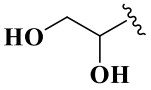
15i	C	N	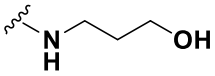	H	C_2H_5	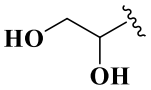
17a	C	N	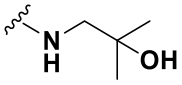	H	C_2H_5	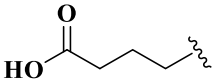
17b	C	N	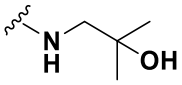	H	C_2H_5	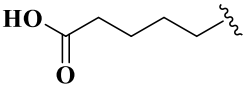
19a	C	N	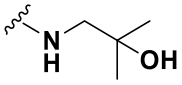	H	C_2H_5	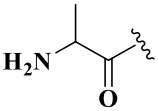
19b	C	N	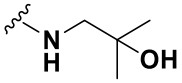	H	C_2H_5	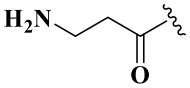

20	C	N	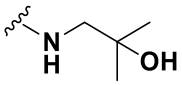	H	C_2H_5	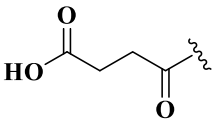

VDR binding affinity.

The VDR binding affinity of synthesized compounds was tested with VDR competitor assay and 1,25$(OH)_2D_3$ was applied as the positive control. All compounds were evaluated for their binding affinity in triplicates at 100 nM. The binding affinity of compounds was exhibited by a reference value to 1,25$(OH)_2D_3$, which is assigned as 100%. Table 1 and Table 2 showed the structure-activity relationships (SARs) for these compounds. Firstly, we focused on the important pharmacophore side chain with C-5 position of pyrrole ring that bearing phenyl-pentane group, the results showed that compounds with the terminal hydrophobic groups in side chain section, such as tert-butoxide (**13a**), tert-butyl (**13b**), trifluoromethyl (**13e**) displayed significant binding affinities. However, introducing flexible hydrophobic substitution n-pentyl group to give compound **13h** resulted in decreased affinity, which suggests that flexible substitution is not preferred in the VDR ligand binding pocket (LBP). Moreover, substitutions of hydrophilic groups, such as 1-hydroxy (**13d**), aminos (**13f-g**), dramatically decreased the binding affinities. By removing the substitution on the pyrrole group C-5 position to C-4 position, compounds **15a-i** were synthesized to explore the influence of substitution position on the binding affinity. Although most compounds displayed decreased binding affinities compared to the pyrrole group C-5 position, compound **15a** bearing

tert-butoxide group showed better activity than the corresponding compound **13a** and turned out to be the most potent molecule. Subsequently, we further investigated the A ring part of target compounds by substitution of the A ring with other hydrophilic groups, such as butanoic acid (**17a**), pentanoic acid (**17b**), alanine (**19a**), β-alanine (**19b**), butanedioic acid (**20**). As a result, no improvement of the binding affinities was detected compared with that of compound **15a**. Meanwhile, carboxylic acid as the terminal hydrophilic group, such as compounds **17a-b** and **20** displayed better binding affinities than that of anime groups (**19a-b**).

Table 2. The affinities of VDR binding and activities of anti-collagen I synthetic at 100 nM.

Compd	Relative VDR binding ability(%)[a]	Anti-collagen I at 100 nM (%)[b]	Compd	Relative VDR binding ability(%)[a]	Anti-collagen I at 100 nM (%)[b]
13a	43±3.2	150±13.6*	**15e**	39±4.8	133±14.5*
13b	45±5.3	159±9.3*	**15f**	—	—
13c	27±4.1	71±7.2	**15g**	—	—
13d	—	—	**15h**	16±1.3	51±5.3

13e	37±2.5	135±15.9*	**15i**	—	—
13f	—	—	**17a**	32±3.9	112±7.8
13g	—	—	**17b**	30±3.2	90±9.2
13h	21±3.5	70±7.9	**19a**	20±2.9	73±4.8
15a	62±4.5	210±20.1*	**19b**	22±4.8	66±5.2
15b	31±2.3	119±7.3*	**20**	30±3.1	80±6.1
15c	—	—	**2**	93±8.5	95±9.2
15d	—	—	**1**	100	100

[a]The values represent the mean ± SD of three independent experiments. 1,25$(OH)_2D_3$ (**1**) is assigned as 100%. 1,25$(OH)_2D_3$ (**1**) and Calcipotriol (**2**) are as the positive control. [b]The values represent the mean ± SD of three independent experiments. 1,25$(OH)_2D_3$ (**1**) is assigned as 100%. 1,25$(OH)_2D_3$ (**1**) and Calcipotriol (**2**) are as the positive control. *P< 0.05 vs. 1,25$(OH)_2D_3$ (**1**).

Transactivation.

To estimate agonistic abilities of the nonsecosteroidal ligands bearing phenyl-pyrrolyl pentane skeleton, a transactivation assay was performed in HEK293 cells using

pGL4.27-*SPP*×3-*Luci* reporter plasmid. Compounds **13a-b**, **15a** and **15e** with strong binding affinities were selected, calcipotriol and 1,25$(OH)_2D_3$ were used as positive control. As shown in Figure 3, all four compounds acted as potent agonists with concentration-dependent transcriptional activity. Among them, compound **15a** was the most potent compound and displayed transcriptional activity at 100 nM, while compounds **13a-b** and **15e** did not reach the optimal transcription level even at 1000 nM. This may due to the interaction of heterodimer partners with VDR, such as nuclear receptor corepressor 1 and steroid receptor coactivator 1, which has an effect on the biological activity of VDR. In addition, a significantly higher increase of transcripts encoding 25-hydroxyvitamin D-24-hydroxylase (*CYP24A1*) by compounds **15a** was showed (Figure S1).

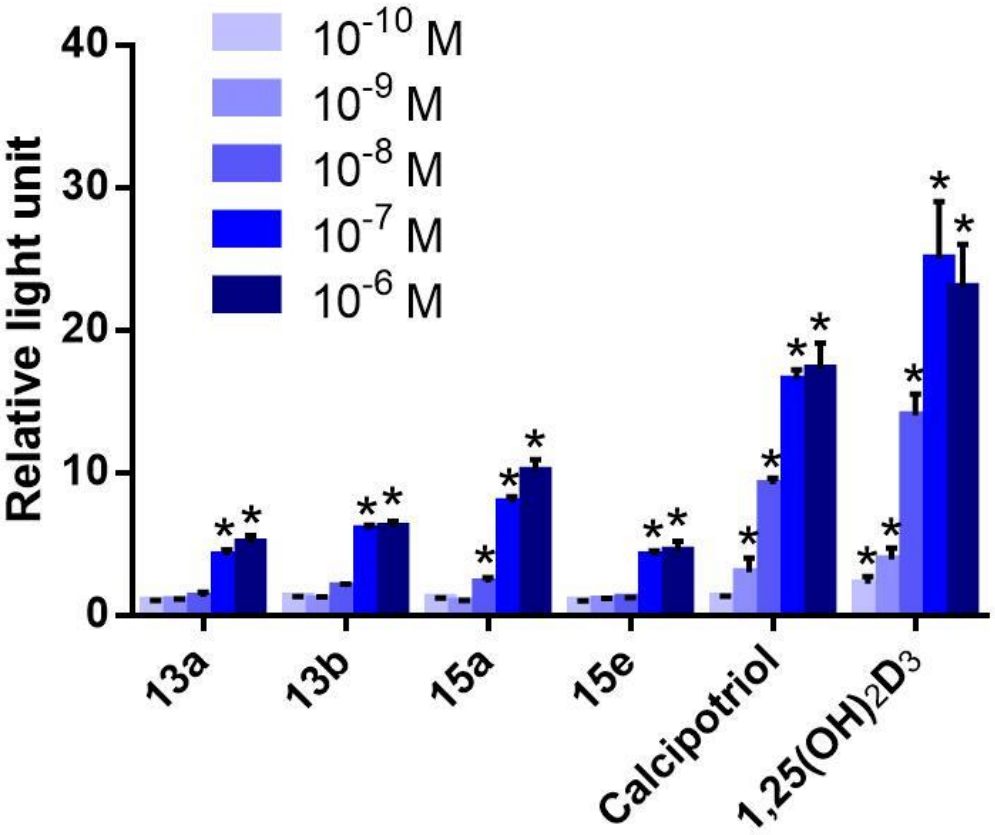

Figure 3. Transcriptional activities of the compounds were examined. HEK293 cells were co-transfected with TK-*SPP* × 3-*Luci* reporter plasmid, pCMX-*Renilla*, pENTER-CMV-*hRXRα* and pCMX−*VDR*. Eight hours after transfection, test compounds, calcipotriol and 1,25$(OH)_2D_3$ were added. 24 hours later, luciferase activity assay was performed using the Dual-Luciferase Assay System. Renilla luciferase activity was as the reference to normalize the firefly luciferase activity. All the experiments were performed three times. *P< 0.05 vs. DMSO.

Anti-collagen I synthetic activities *in vitro*.

Liver fibrosis is characterized by the replacement of functional hepatic tissue with

highly cross-linked collagen I-rich ECM and TGFβ1 is recognized as one of the most potent pro-fibrotic modulator responsible for collagen I synthesis. Consequently, inhibiting the production of collagen I induced by TGFβ1 is an effective strategy to against fibrotic progress. To examined the anti-fibrotic effects of all target compounds, an stable and unlimited source of human HSCs, LX-2 cells, were employed as a valuable cell model to study human hepatic fibrosis.[43] Calcipotriol and 1,25$(OH)_2D_3$ were applied as positive control (Table 2). Compared with calcipotriol and 1,25$(OH)_2D_3$, seven of the synthesized analogues (**13a-b**, **13e**, **15a-b**, **15e**, and **17a**) at the concentration of 100 nM, which was little cytotoxic to LX-2 (Table S1), demonstrated more effective inhibitory properties against collagen I synthesis, with the values at the range of 112-210%, and six compounds (1**3c**, **13h**, **17b**, **19a-b**, and **20**) displayed an equivalent inhibitory potency. This discrepancy between binding affinity and agonistic activity could be interpreted by the interactions between the cofactors and VDR ligand complex. It is required AF-2 transactivation motif of VDR to interacts with cofactors such as VDR interacting proteins (DRIPs) for the VDR transcriptional activation.[37-39] Table 2 highlights the important SARs features of inhibitory potencies. Similar to the SARs of binding affinities, **13a-b** and **13e** bearing terminal hydrophobic groups in the side chain section also displayed significant inhibitory activities. In addition, compound **13h**, which showed decreased binding affinity compared with other compounds bearing terminal hydrophobic groups as described above, was also only moderately active. Replacement of hydrophobic groups with hydrophilic groups, such as 1-hydroxy (**13d**), aminos (**13f-g**), dramatically

weakened the inhibitory activities. On this point, it could be proved that the inhibitory activities of synthesized compounds are positively correlative with VDR binding affinities. Varying the position of the substitution from pyrrole group C-5 position to C-4 had dramatically effects on inhibitory activities. As likely as the binding affinities, compound **15a** showed better activity than the corresponding compound **13a** and turned out to be the most potent molecule. In addition, all compounds varying propane-1.2-diol to other hydrophilic groups displayed moderate inhibitor activities against collagen I synthesis and had no better results than **15a**. Meanwhile, carboxylic acid as the terminal hydrophilic group, such as compounds **17a-b** and **20** displayed better inhibitory activities than that of anime groups (**19a-b**).

Effects on the expression of collagen I and α-SMA in LX-2 cells.

The anti-fibrotic activities of selected compounds **13a**, **13b**, **15a**, and **15e**, which displayed optimal property on binding affinities and anti-collagen I synthetic activities, were analyzed using western blot and Q-PCR assays. The increased expression of collagen I and α-SMA is the markers of activated HSCs[3]. As described above, liver fibrosis, regardless of its cause, is featured by progressive accumulation of ECM proteins and the mainly component is collagen I. Moreover, the α-SMA-positive myofibroblasts is considered as the key promoter in the progression of liver fibrosis. Collagen I alpha 1 (*COL1A1*) is the direct target of VDR[20], in addition, a-SMA and collagen I are both upregulated by TGFβ1 in HSCs. Therefore, the expression of α-SMA

and collagen I were selected to determine the anti-fibrotic activities of selected compounds. As shown in Figure 4C and D, the activity of these molecules was significantly affected by the pyrrole group substitution position, compounds **15a** and **15e** (C-4 substitution) at the concentration of 100 nM significantly reduced α-SMA and collagen I protein levels in TGFβ1-treated LX-2 cells, while compounds **13a** and **13b** (C-4 substitution) exhibited no significant influence on *ACTA2* expression. Compared with the hydroxyl group contained analog **15a**, the molecules **15e** showed less activity, which suggest that hydroxyl group in the side chain terminal is essential. Q-PCR results

(Figure 4A and B) showed that compound **15a** significantly down-regulated *COL1A1* and *ACTA2* mRNA expression. Moreover, compared with positive control calcipotriol and 1,25$(OH)_2D_3$, compound **15a** showed more effective inhibitory potency against *COL1A1*

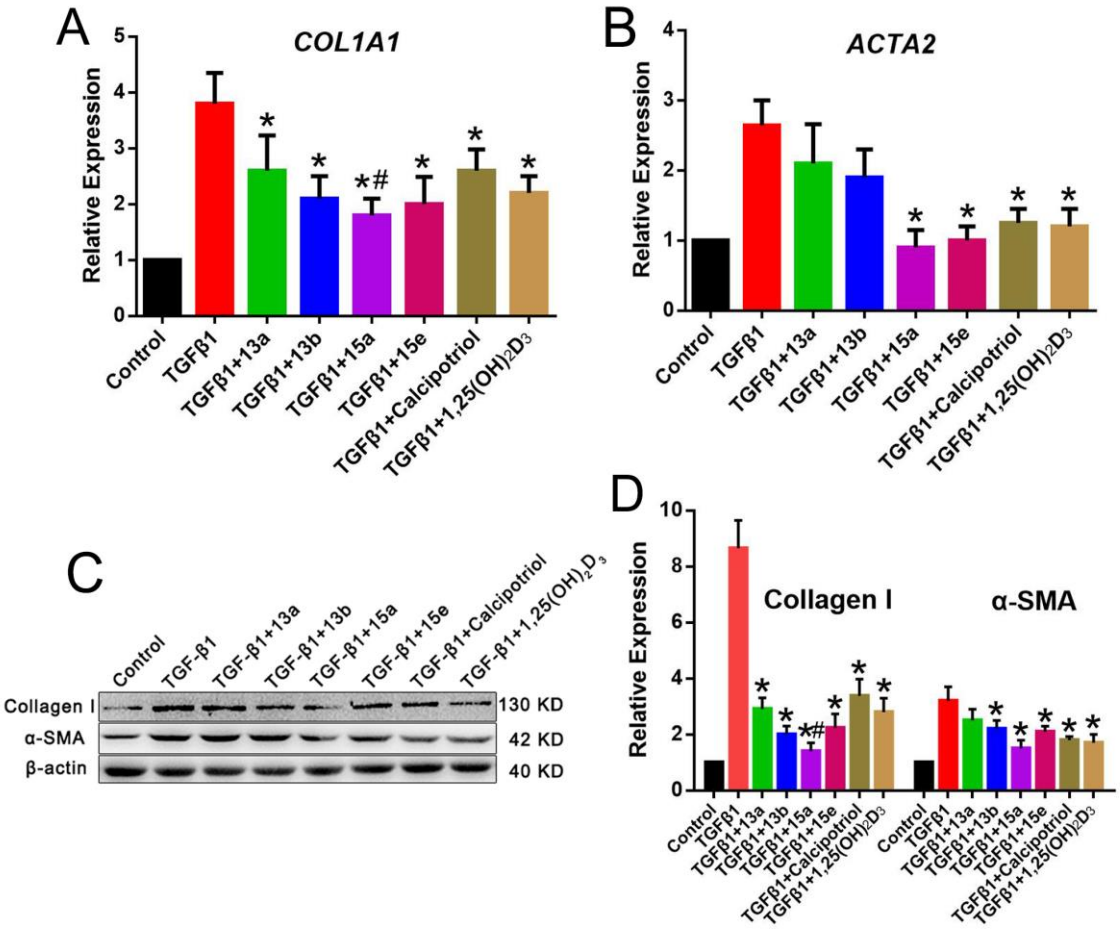

mRNA expression. The results impel us continuously to test the anti-fibrotic effect of these compounds.

Figure 4. Effects of compounds on activation of LX-2 cells. LX-2 cells were cultured with compounds, calcipotriol or 1,25$(OH)_2D_3$ for 24 hours at 100 nM. (A and B) The expression levels of *ACTA2* and *COL1A1* were measured by Q-PCR. (C and D)

Expression of α-SMA and collagen I on LX-2 cells was determined by western blot. The representative gel electrophoresis bands are shown (C), and expression levels of proteins were normalized to the expression of β-actin (D). Densitometry data are shown as mean ± SD. *P< 0.05 vs. TGFβ1, #P< 0.05 vs. TGFβ1+Calcipotriol.

15a inhibited activation of LX-2 cells through VDR.

VDR is recognized the potential therapy target for liver fibrosis and the above-mentioned results suggested the compounds may be VDR agonists. To confirm that compound **15a** repressed fibrotic gene expression via VDR, RNA interference (RNAi) was used in LX-2 cells. Loss of VDR abolished **15a**-mediated repression of collagen I and α-SMA expression was shown in Figure 5. These data demonstrated that compound **15a** exerts its repressing effect on HSCs activation through interaction with VDR.

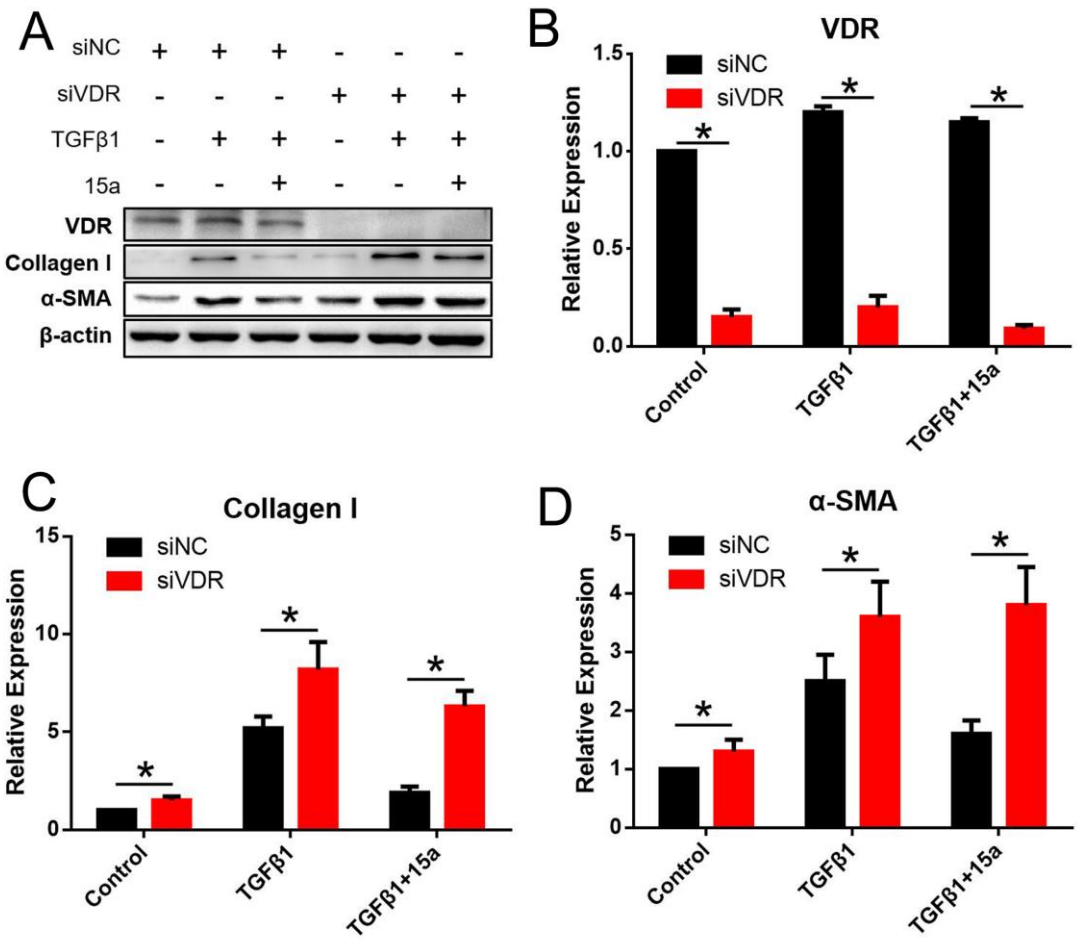

Figure 5. 15a inhibited activation of LX-2 cells via VDR. (A) *VDR*-specific (siVDR) or negative control (siNC) siRNA-transfected LX-2 cells were treated with **15a** (100 nM), TGFβ1 (1 ng/mL), or TGFβ1 plus **15a** for 24 hours. The expression of VDR, α-SMA and collagen I on LX-2 cells was tested by western blot. The representative gel electrophoresis bands are shown. (B, C and D) Expression levels of VDR, collagen I and α-SMA were normalized to the expression of β-actin. The quantified densitometry data are shown as mean ± SD. *P< 0.05.

Effects on suppressing the expression of α-SMA in CCl_4-induced hepatic fibrosis

mice.

Based on *in vitro* results, compound **15a** was selected for further studies *in vivo*. To explore whether compound **15a** could repress the expression of fibrotic gene and inhibit hepatic fibrogenesis *in vivo*, CCl_4 was used to induce liver fibrosis by intraperitoneal (IP) injection in C57BL/6J mice. The anti-fibrotic property of compound **15a** was determined by histological examination. As shown in Figure 6, consistent with the above studies *in vitro*, oral administration of compound **15a** to CCl_4-treated mice reduced α-SMA levels in the liver tissues according to Q-PCR and IHC staining. In addition, compound **15a** also increased the mRNA levels of *Cyp24a1*, suggesting **15a** inhibits fibrotic progress through agitating VDR (Figure S2).

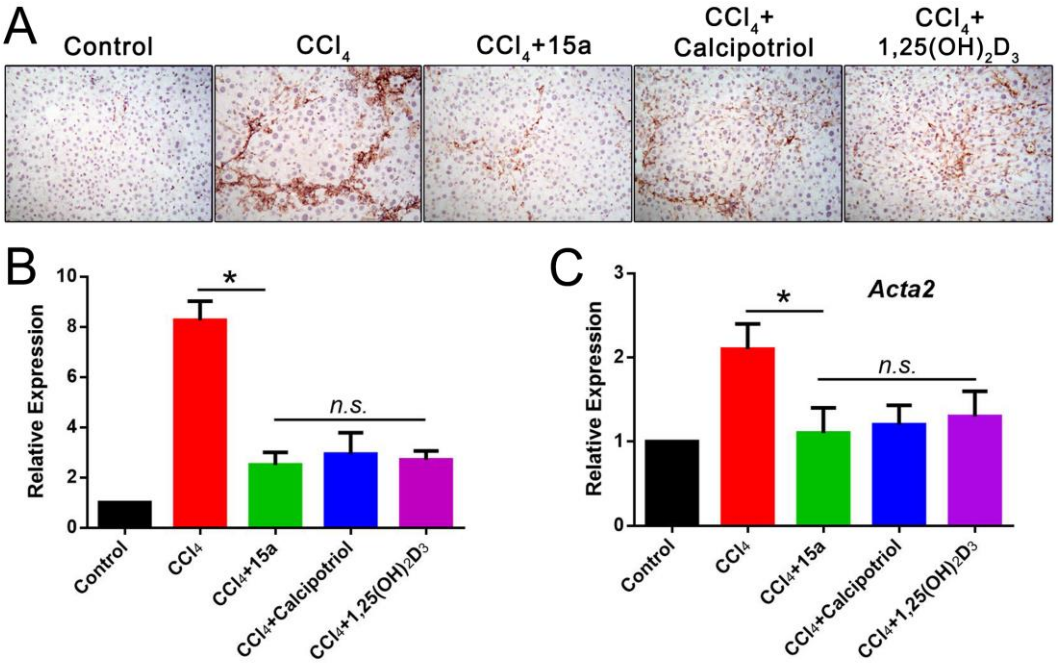

Figure 6. **15a** suppressed the expression of α-SMA in CCl_4-induced hepatic fibrosis lesions and protected the liver from impairment. Mice (n=5 in each group) received either

DMSO or CCl_4 (0.5 mL/kg body weight) intraperitoneally for three weeks before intragastric administration of **15a**, calcipotriol, $1,25(OH)_2D_3$ (20 μg/kg body weight) or DMSO. (A) α-SMA expression in the injured liver was tested by immunohistochemistry (×200). (B) The expression levels of α-SMA were quantified using Image-Pro Plus 6.0. Data are shown as mean ± SD. $^{*}P< 0.05$ vs. CCl_4. (C) Expression of *Acta2* in the injured liver was examined by Q-PCR (mean ± SD. $^{*}P<0.05$).

Effects on suppressing the expression of collagen in CCl_4-induced hepatic fibrosis mice.

In addition, we measured collagen content to further examine the anti-fibrotic effect of compound **15a**. Histopathologically, compound **15a** treatment resulted in the inhibition of collagen accumulation in CCl_4 mice liver based on H&E and Masson's trichrome staining (Figure 7A). The amounts of hepatic hydroxyproline in liver tissue were estimated, which was a major component of the collagen. As shown in Figure 7B, treatment of compound **15a** had a significant reduction in hydroxyproline content, with slightly stronger potency than positive control calcipotriol and $1,25(OH)_2D_3$. Moreover, mRNA levels of *Col1α1* was elevated in the liver fibrosis models, the results showed that the expression of *Col1α1* was also reduced by compound **15a** treatment (Figure 7C). These results suggest that compound **15a** treatment prevents CCl_4-induced liver injury and hepatic fibrosis.

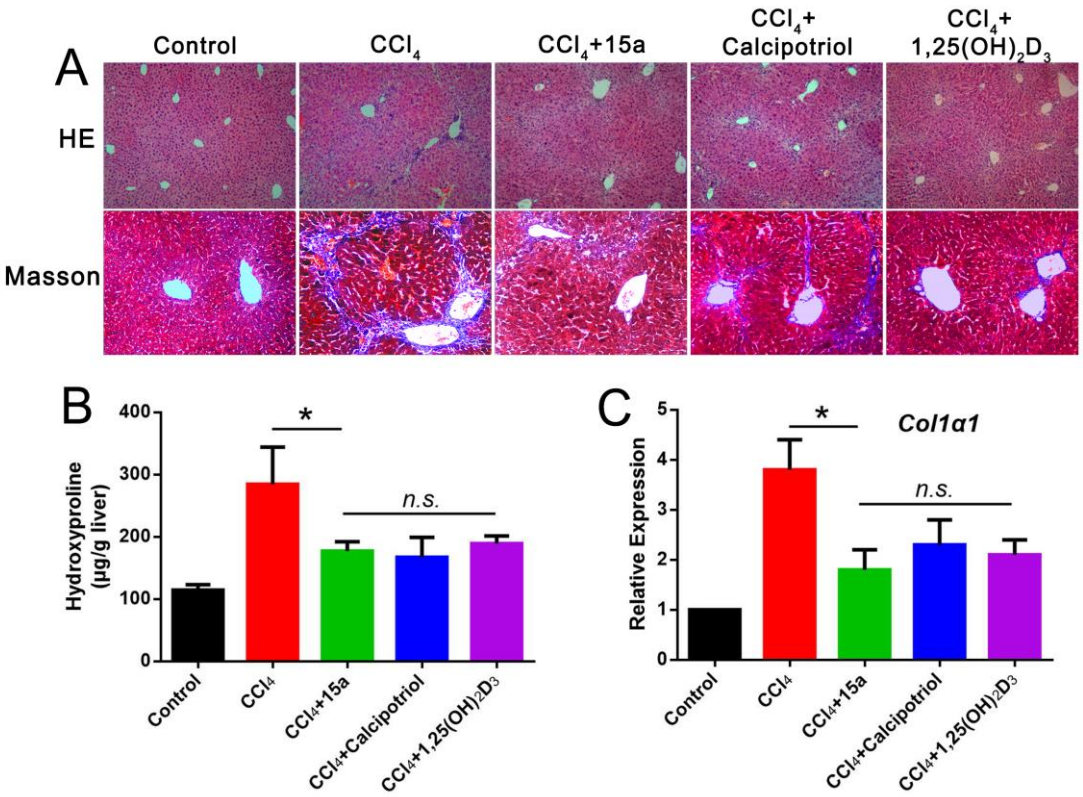

Figure 7. **15a** inhibited the CCl_4-induced hepatic lesions and collagen deposition. Mice (n=5 in each group) received either DMSO or CCl_4 (0.5 mL/kg body weight) intraperitoneally for three weeks before intragastric administration of **15a**, calcipotriol, $1,25(OH)_2D_3$ (20 μg/kg body weight) or DMSO. (A and B) CCl_4-induced hepatic fibrosis lesions were examined by H&E staining (×100), the collagen deposition was determined by Masson's trichrome staining (×200) and hydroxyl proline measurement (mean ± SD. *P＜0.05 vs. CCl_4). (C) Expression of *Col1a1* in the injured liver was examined by Q-PCR (mean ± SD. *P＜0.05).

Effects on liver function and serum calcium of fibrotic models.

Serum alanine transaminase (ALT), aspartate transaminase (AST), and total bile acid

(TBA) levels are commonly measured clinically as biomarkers for liver health.[40] Significantly elevated levels of AST, ALT and TBA often suggest the existence of liver damage. As shown in Figure 8A, B and C, the levels of AST, ALT and TBA were significantly decreased in compound **15a**-treated mice as compared with control animals. Moreover, compound **15a** displayed better results than positive control calcipotriol and 1,25$(OH)_2D_3$, which are very promising for the reduction of liver damage. To determine the effect of novel designed nonsecosteroidal analogs on inducing hypercalcemic, calcium concentration was measured by calcemic activity assay *in vivo*. Ma et al. reported that nonsecosteroidal VDR modulators showed poor activity in intestinal cells.[41] Moreover, the nonsecosteroidal compound has the ability to activate VDR and is weak in binding to vitamin D-binding proteins, so that it does not accumulate excessively in the intestinal, resulting in no excessive calcium absorption.[29] In our study, compound **15a** displayed small impact on the expression of intestinal *Trpv6*, which is a VDR target gene involved in calcium metabolism (Figure S3). As shown in Figure 8D, compared with calcipotriol and 1,25$(OH)_2D_3$, there was no significant effect on serum calcium when treated with compound **15a** in mice, which suggests that nonsecosteroidal analog **15a** results in a high dissociation of anti-fibrotic potency from calcemic effects.

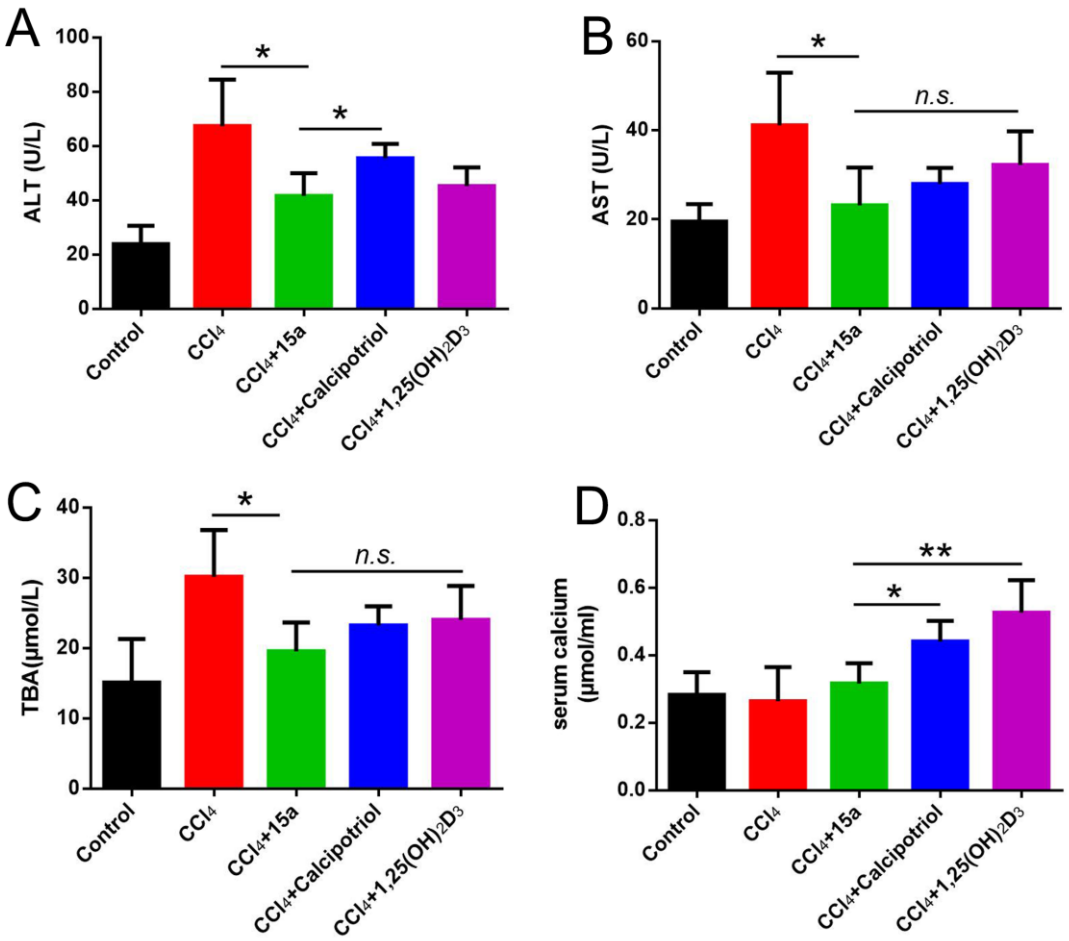

Figure 8. **15a** protected the liver from impairment. Mice (n=5 in each group) received either DMSO or CCl_4 (0.5 mL/kg body weight) intraperitoneally for three weeks before intragastric administration of **15a**, calcipotriol, $1,25(OH)_2D_3$ (20 μg/kg body weight) or DMSO. (A, B, and C) The serum levels of ALT, AST and TBA were determined. (D) The serum calcium concentration was determined by calcium assay kit (mean ± SD. *P<0.05, **P<0.01).

In Vivo Pharmacokinetics Study.

Pharmacokinetic studies of compound **15a** and $1,25(OH)_2D_3$ were performed in rats.

The results were shown in Table S3. Oral bioavailability of compound **15a** was 29.32% and t½ value was 6.57 h after oral administration. **15a** displayed similiar bioavailability compared with 1,25$(OH)_2D_3$, whose bioavailability was 30.83% after oral administration. However, the t½ value of **15a** was a little smaller compared with 1,25$(OH)_2D_3$, whose t½ value was 7.55 h after oral administration. This maybe because nonsecosteroidal VDR agonist did not combined with vitamin D binding protein,[29] then the metabolism of **15a** is slightly faster. Still, the results suggested that **15a** could possess therapeutic potentials for treatment of liver fibrosis.

Docking analyse.

In this study, we have performed VDR binding assay, transactivation assay, as well as knocking down VDR gene to prove that compound **15a** repress fibrotic gene expression via VDR. To clarify the detailed interactions of VDR and the most promising compound **15a**, molecular docking study was made on the basis of complexation crystallographic structure of LG190178 and VDR (PDB code: 2ZFX). Using software Discovery Studio 3.0, compound **15a** was manually docked into the crystal structure of VDR. Figure 9A showed the conformations superposition of compound **15a** and the natural ligand 1,25$(OH)_2D_3$. Figure 9B showed the conformations superposition of compound **15a** and YR301. Docking analyses The results demonstrated that the A ring part and side chain of compound **15a** exhibited similar conformations to those detected in the presence of YR301 and 1,25$(OH)_2D_3$. As shown in Figure 9C, the hydroxyl group of compound **15a**

in the side chain could form the hydrogen-bonding interactions with His 301 and His 393, which are same to 1,25$(OH)_2D_3$ bound to the hVDR LBD complex. However, the A ring part of 1,25$(OH)_2D_3$ bound with Ser 233, Arg 270, Tyr 139, and Ser 274, while compound **15a** only form hydrogen-bonding interaction with Arg 270 by 2-OH. This may affect the interactions of compound **15a** to VDR and result in reducing binding affinity.

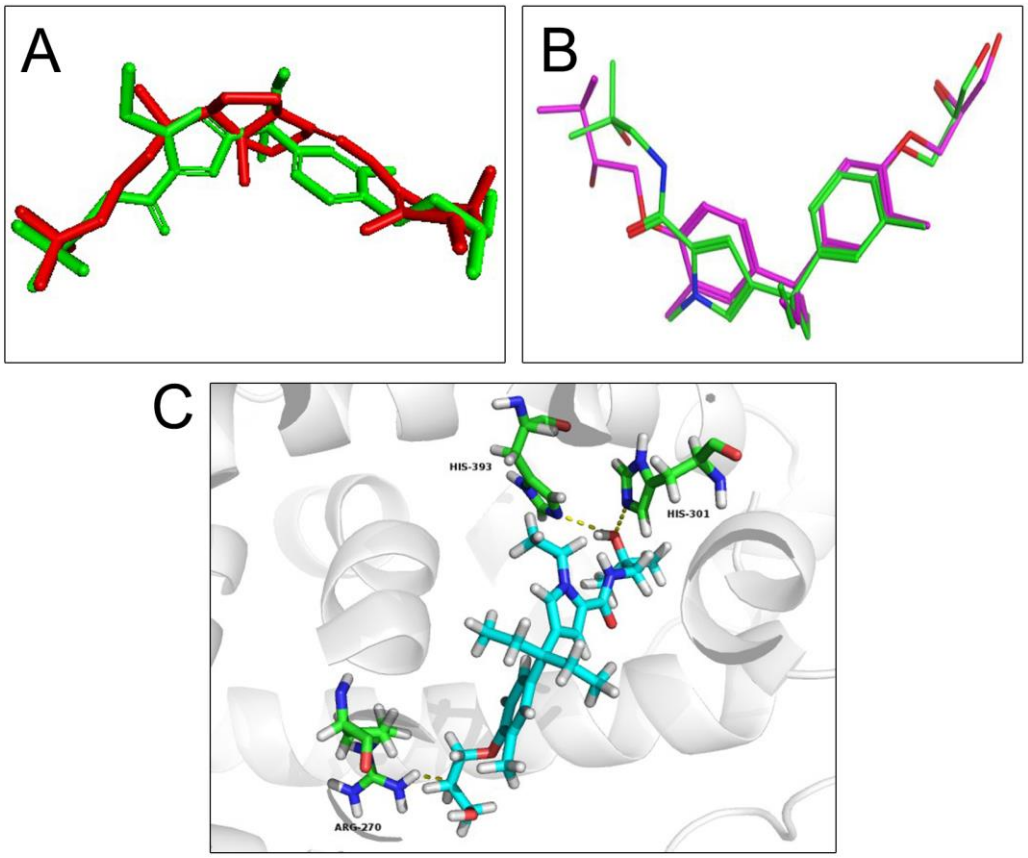

Figure 9. (A) Superposition of compounds **15a** and 1,25$(OH)_2D_3$. Compound **15a** is depicted in green and 1,25$(OH)_2D_3$ is depicted in red. (B) Superposition of compounds **15a** and YR301. **15a** is depicted in green and YR301 is in pink. (C) Docking structure of the complex **15a**-VDR. The ligands are exhibited in stick representation, carbon is

depicted in cyan and oxygen atoms in red. The hydrogen bonds that formed between ligands and VDR are exhibited as yellow dashed lines.

CONCLUSION

In conclusion, the design, synthesis, and biological assessment of nonsecosteroidal derivatives with phenyl-pyrrolyl pentane skeleton have been described in this manuscript. The selected compounds are act as VDR agonists for effectively preventing the progression of liver fibrosis. The analysis of SAR directed the synthesis of the derivative **15a**, which may be a strong inhibitor for collagen I synthesis. Further exploration demonstrated that compound **15a** had higher inhibitory activity on fibrotic gene expression and collagen deposition. Histological examination results displayed that compound **15a** treatment prevented hepatic fibrosis induced by CCl_4 injections in mice. More importantly, compound **15a** can display better results for the reduction of liver damage without significant change on serum calcium, which can be induced by positive control calcipotriol and $1,25(OH)_2D_3$. This work supports that using nonsecosteroidal VDR modulators may be applied for the treatment of hepatic fibrosis due to there is still no effective therapeutic strategies at present.

EXPERIMENTAL SECTION

Chemistry.

General Information.

Commercially available reagents and solvents were used without further purification. Column chromatography was carried out on Merck silica gel 60 (200-300 mesh). ^{1}H and ^{13}C NMR spectra were recorded with 300 MHz spectrometers in the indicated solvents (TMS as internal standard). Chemical shifts were reported in parts per million (ppm, δ) downfield from tetramethylsilane. Proton coupling patterns are described as singlet (s), doublet (d), triplet (t), quartet (q), double doublet (dd), multipet (m) and broad (br). Purity of all tested compounds was ≥95%, as estimated by HPLC analysis. The major peak of the compounds analyzed by HPLC accounted for ≥95% of the combined total peak area when monitored by a UV detector at 254 nm. Low-resolution mass spectra (LR-MS) and High-resolution mass spectra (HR-MS) were measured on Agilent QTOF 6520.

General Procedures.

Ethyl-5-(3-(4-benzyloxy-3-methylphenyl)pentan-3-yl)-1H-pyrrole-2-carboxylate (8a). $BF_3 \cdot Et_2O$ (13 mL, 105 mmol) was added dropwise to a solution of intermediate **7** (13 g, 46 mmol) and ethyl-1H-pyrrole-2-carboxylate (7.1 g, 51 mmol) in dichloromethane (20 mL) at 0°C. The mixture was stirred for 1 h at 25°C. Then the solution was added H_2O and organic phase was separated. The organic phases were washed with brine and dried over anhydrous Na_2SO_4 and evaporated. The residue was purified by column chromatography with petroleum ether/ethyl acetate (20/1, v/v) to give

compound **8a** as yellow solid (13.5 g, 73% yield).

Ethyl-4-(3-(4-(benzyloxy)-3-methylphenyl)pentan-3-yl)-1H-pyrrole-2-carboxylate (8b). By the same manner as described for the preparation of **8a**, the intermediate **8b** was prepared from the intermediate **4** and purified by silica gel chromatography with petroleum ether/ethyl acetate (12/1, v/v). Yield: 44%.

Ethyl-5-(3-(4-(benzyloxy)-3-methylphenyl)pentan-3-yl)-1-ethyl-1H-pyrrole-2-carboxylate (9a). To a solution of compound **8a** (4.05 g, 10 mmol) in DMF (5 mL), NaH (288 mg, 12 mmol) was added portion-wise at 0°C. After stirring for 0.5 h, ethyl iodide (1.25 g, 8 mmol) was added. The reaction mixture was stirred at 25°C for 2 h and then H_2O (20 mL) was added drop-wise followed by ethyl acetate (10 mL). The organic phase was separated and the aqueous phase was extracted with ethyl acetate. The combined organic phases were washed with H_2O, brine and then dried over anhydrous Na_2SO_4 and evaporated. The residue was purified by column chromatography with petroleum ether/ethyl acetate (20/1, v/v) to give compound **9a** as yellow oil (3.57 g, 82.4% yield).

Ethyl-4-(3-(4-(benzyloxy)-3-methylphenyl)pentan-3-yl)-1-ethyl-1H-pyrrole-2-carboxylate (9b). By the same manner as described for the preparation of **9a**, the intermediate **9b** was prepared from the intermediate **8b** and purified by silica gel chromatography with petroleum ether/ethyl acetate (20/1, v/v). Yield: 85%.

Ethyl-1-ethyl-5-(3-(4-hydroxy-3-methylphenyl)pentan-3-yl)-1H-pyrrole-2-carboxylate (10a). To a solution of intermediate **9a** (2.0 g, 4.6 mmol) in methanol (20 mL), Pd/C

(0.2 g) and ammonium formate (2.9 g, 46 mmol) was added. The reaction mixture was stirred at 25°C overnight. The precipitate was filtered offH_2O (100 mL) and ethyl acetate (50 mL) was added to the solution. The organic phase was separated and the aqueous phase was extracted with ethyl acetate. The combined organic phases were washed with brine, then dried over anhydrous Na_2SO_4 and evaporated to give compound **10a** as white solid (1.55 g, 98% yield).

Ethyl-1-ethyl-4-(3-(4-hydroxy-3-methylphenyl)pentan-3-yl)-1H-pyrrole-2-carboxylate (10b). By the same manner as described for the preparation of **10a**, the intermediate **10b** was prepared from the intermediate **9b**. Yield: 97%.

1-ethyl-5-(3-(4-hydroxy-3-methylphenyl)pentan-3-yl)-1H-pyrrole-2-carboxylic acid (11a). The intermediate **10a** (351 mg, 1 mmol) was dissolved in ethanol (6 mL), treated with KOH (168 mg, 3 mmol) in H_2O, and the reaction mixture was stirred at 80 °C for 5 h. The solution was diluted with H_2O (20 mL) and the pH value was adjusted to about 3-4 using 1 M HCl. Then it was extracted with ethyl acetate. The aqueous phase was extracted with ethyl acetate. The combined organic phases were washed with brine and then dried over anhydrous Na_2SO_4 and evaporated. The residue was purified by column chromatography with petroleum ether/ethyl acetate (10/1, v/v) to give the intermediate **11a** as yellow oil (307 mg, 94%).

1-ethyl-4-(3-(4-hydroxy-3-methylphenyl)pentan-3-yl)-1H-pyrrole-2-carboxylic acid (11b). By the same manner as described for the preparation of **11a**, the intermediate

11b was prepared from the intermediate **10b**. Yield: 95%.

1-ethyl-N-(2-hydroxy-2-methylpropyl)-5-(3-(4-hydroxy-3-methylphenyl)pentan-3-yl)-1H-pyrrole-2-carboxamide (12a). To a solution of compound **11a** (250 mg, 0.61 mmol) in CH_2Cl_2 (10 mL) was added Et_3N (255 μL, 1.83 mmol), followed by1-amino-2-methylpropan-2-ol (153 mg, 1.22 mmol), EDCI (175 mg, 0.92 mmol) and HOBt (124 mg, 0.92 mmol). The reaction mixture was stirred at 25 °C overnight and then poured into H_2O. The solution was extracted with CH_2Cl_2, and aqueous phase was extracted with CH_2Cl_2. The combined organic phases were washed with H_2O, brine, then dried over anhydrous Na_2SO_4 and evaporated. The residue was purified by column chromatography with petroleum ether/ethyl acetate (4/1, v/v) to give compound **12a** as white solid (233 mg, 82% yield).

1-ethyl-5-(3-(4-hydroxy-3-methylphenyl)pentan-3-yl)-N-neopentyl-1H-pyrrole-2-carboxamide (12b). By the same manner as described for the preparation of **12a**, the intermediate **12b** was prepared from the intermediate **11a**. Yield: 78%.

N-(cyclopropylmethyl)-1-ethyl-5-(3-(4-hydroxy-3-methylphenyl)pentan-3-yl)-1H-pyrrole-2-carboxamide (12c). By the same manner as described for the preparation of **12a**, the intermediate **12c** was prepared from the intermediate **11a**. Yield: 57%.

Methyl(1-ethyl-5-(3-(4-hydroxy-3-methylphenyl)pentan-3-yl)-1H-pyrrole-2-carbonyl)glycinate (12d). By the same manner as described for the preparation of **12a**, the intermediate **12d** was prepared from the intermediate **11a**. Yield: 57%.

1-ethyl-5-(3-(4-hydroxy-3-methylphenyl)pentan-3-yl)-N-(2-hydroxyethyl)-1H-pyrrole-2-carboxamide (12d-OH). To a solution of **12d** (114 mg, 0.23 mmol) in ethyl acetate (10 mL), $LiAlH_4$ (13 mg, 0.35 mmol) was added portion-wise at 0 °C. The reaction mixture was stirred at 25 °C for 1 h and then added H_2O (10 mL). The solution was extracted with ethyl acetate, and aqueous phase was extracted with ethyl acetate. The combined organic phases were washed with brine and then dried over anhydrous Na_2SO_4 and evaporated. The residue was purified by column chromatography with petroleum ether/ethyl acetate (1/1, v/v) to give compound **12d-OH** as white solid (100 mg, 96% yield).

1-ethyl-5-(3-(4-hydroxy-3-methylphenyl)pentan-3-yl)-N-(2,2,2-trifluoroethyl)-1H-pyrrole-2-carboxamide (12e). By the same manner as described for the preparation of **12a**, the intermediate **12e** was prepared from the intermediate **11a**. Yield: 45%.

N-(3-(dimethylamino)propyl)-1-ethyl-5-(3-(4-hydroxy-3-methylphenyl)pentan-3-yl)-1H-pyrrole-2-carboxamide (12f). By the same manner as described for the preparation of **12a**, the intermediate **12f** was prepared from the intermediate **11a**. Yield: 68%.

N-(2-(dimethylamino)ethyl)-1-ethyl-5-(3-(4-hydroxy-3-methylphenyl)pentan-3-yl)-1H-pyrrole-2-carboxamide (12g). By the same manner as described for the preparation of **12a**, the intermediate **12g** was prepared from the intermediate **11a**. Yield: 62%.

1-ethyl-5-(3-(4-hydroxy-3-methylphenyl)pentan-3-yl)-N-pentyl-1H-pyrrole-2-carboxamide (12h). By the same manner as described for the preparation of **12a**, the

intermediate **12g** was prepared from the intermediate **11a**. Yield: 87%.

5-(3-(4-(2,3-dihydroxypropoxy)-3-methylphenyl)pentan-3-yl)-1-ethyl-N-(2-hydroxy-2-methylpropyl)-1H-pyrrole-2-carboxamide (13a). To a solution of intermediate **12a** (386 mg, 1 mmol) in DMF, NaH (80 mg, 2 mmol) was added portion-wise at 0 °C. The reaction mixture was stirred at 0 °C for 1 h and then added glycidol (0.1 mL, 1.5 mmol). The reaction mixture was moved to 80 °C for 5 h and then added H_2O (10 mL).The solution was extracted with ethyl acetate, and aqueous phase was extracted with ethyl acetate. The combined organic phases were washed with brine and then dried over anhydrous Na_2SO_4 and evaporated. The residue was purified by column chromatography (CH_2Cl_2/CH_3OH = 50/1) to give compound **13a** as white solid (245 mg, 53% yield).

5-(3-(4-(2,3-dihydroxypropoxy)-3-methylphenyl)pentan-3-yl)-1-ethyl-N-neopentyl-1H-pyrrole-2-carboxamide (13b). By the same manner as described for the preparation of **13a**, compound **13b** was prepared from the intermediate **12b**. Yield: 87%.

N-(cyclopropylmethyl)-5-(3-(4-(2,3-dihydroxypropoxy)-3-methylphenyl)pentan-3-yl)-1-ethyl-1H-pyrrole-2-carboxamide (13c). By the same manner as described for the preparation of **13a**, compound **13c** was prepared from the intermediate **12c**. Yield: 44%.

5-(3-(4-(2,3-dihydroxypropoxy)-3-methylphenyl)pentan-3-yl)-1-ethyl-N-(2-hydroxyethyl)-1H-pyrrole-2-carboxamide (13d). By the same manner as described for the preparation of **13a**, compound **13d** was prepared from the intermediate **12d-OH**. Yield: 35%.

5-(3-(4-(2,3-dihydroxypropoxy)-3-methylphenyl)pentan-3-yl)-1-ethyl-N-(2,2,2-trifluoroethyl)-1H-pyrrole-2-carboxamide (13e). By the same manner as described for the preparation of **13a**, compound **13e** was prepared from the intermediate **12e**. Yield:68%.

5-(3-(4-(2,3-dihydroxypropoxy)-3-methylphenyl)pentan-3-yl)-N-(3-(dimethylamino)propyl)-1-ethyl-1H-pyrrole-2-carboxamide (13f). By the same manner as described for the preparation of **13a**, compound **13f** was prepared from the intermediate **12f**. Yield: 78%.

N-(3-(diethylamino)propyl)-5-(3-(4-(2,3-dihydroxypropoxy)-3-methylphenyl)pentan-3-yl)-1-ethyl-1H-pyrrole-2-carboxamide (13g). By the same manner as described for the preparation of **13a**, compound **13g** was prepared from the intermediate **12g**. Yield: 64%.

5-(3-(4-(2,3-dihydroxypropoxy)-3-methylphenyl)pentan-3-yl)-1-ethyl-N-pentyl-1H-pyrrole-2-carboxamide (13h). By the same manner as described for the preparation of **13a**, compound **13h** was prepared from the intermediate **12h**. Yield: 96%.

4-(3-(4-(2,3-dihydroxypropoxy)-3-methylphenyl)pentan-3-yl)-1-ethyl-N-(2-hydroxy-2-methylpropyl)-1H-pyrrole-2-carboxamide (14a). By the same manner as described for the preparation of **12a**, the intermediate **14a** was prepared from the intermediate **11b**. Yield: 53%.

1-ethyl-4-(3-(4-hydroxy-3-methylphenyl)pentan-3-yl)-N-neopentyl-1H-pyrrole-2-c

arboxamide (14b). By the same manner as described for the preparation of **12a**, the intermediate **14b** was prepared from the intermediate **11b**. Yield: 76%.

N-(cyclopropylmethyl)-1-ethyl-4-(3-(4-hydroxy-3-methylphenyl)pentan-3-yl)-1H-pyrrole-2-carboxamide (14c). By the same manner as described for the preparation of **12a**, the intermediate **14c** was prepared from the intermediate **11b**. Yield: 42%.

Methyl(1-ethyl-4-(3-(4-hydroxy-3-methylphenyl)pentan-3-yl)-1H-pyrrole-2-carbonyl)glycinate (14d). By the same manner as described for the preparation of **12a**, the intermediate **14d** was prepared from the intermediate **11b**. Yield: 89%.

1-ethyl-4-(3-(4-hydroxy-3-methylphenyl)pentan-3-yl)-N-(2-hydroxyethyl)-1H-pyrrole-2-carboxamide (14d-OH). By the same manner as described for the preparation of **12d-OH**, the intermediate **14d-OH** was prepared from the intermediate **14d**. Yield: 87%.

1-ethyl-4-(3-(4-hydroxy-3-methylphenyl)pentan-3-yl)-N-(2,2,2-trifluoroethyl)-1H-pyrrole-2-carboxamide (14e). By the same manner as described for the preparation of **12a**, the intermediate **14e** was prepared from the intermediate **11b**. Yield: 53%.

Methyl(1-ethyl-4-(3-(4-hydroxy-3-methylphenyl)pentan-3-yl)-1H-pyrrole-2-carbonyl)alaninate (14f). By the same manner as described for the preparation of **12a**, the intermediate **14f** was prepared from the intermediate **11b**. Yield: 32%.

1-ethyl-4-(3-(4-hydroxy-3-methylphenyl)pentan-3-yl)-N-(1-hydroxypropan-2-yl)-1H-pyrrole-2-carboxamide (14f-OH). By the same manner as described for the

preparation of **12d-OH**, the intermediate **14f-OH** was prepared from the intermediate **14f**. Yield: 46%.

Methyl(1-ethyl-4-(3-(4-hydroxy-3-methylphenyl)pentan-3-yl)-1H-pyrrole-2-carbonyl)valinate (14g). By the same manner as described for the preparation of **12a**, the intermediate **14g** was prepared from the intermediate **11b**. Yield: 49%.

1-ethyl-N-(1-hydroxy-3-methylbutan-2-yl)-4-(3-(4-hydroxy-3-methylphenyl)pentan-3-yl)-1H-pyrrole-2-carboxamide (14g-OH). By the same manner as described for the preparation of **12d-OH**, the intermediate **14g-OH** was prepared from the intermediate **14g**. Yield: 61%.

1-ethyl-4-(3-(4-hydroxy-3-methylphenyl)pentan-3-yl)-N-pentyl-1H-pyrrole-2-carboxamide (14h). By the same manner as described for the preparation of **12a**, the intermediate **14h** was prepared from the intermediate **11b**. Yield: 81%.

1-ethyl-4-(3-(4-hydroxy-3-methylphenyl)pentan-3-yl)-N-(3-hydroxypropyl)-1H-pyrrole-2-carboxamide (14i). By the same manner as described for the preparation of **12a**, the intermediate **14i** was prepared from the intermediate **11b**. Yield: 72%.

4-(3-(4-(2,3-dihydroxypropoxy)-3-methylphenyl)pentan-3-yl)-1-ethyl-N-(2-hydroxy-2-methylpropyl)-1H-pyrrole-2-carboxamide (15a). By the same manner as described for the preparation of **13a**, compound **15a** was prepared from the intermediate **14a**. Yield: 67%.

4-(3-(4-(2,3-dihydroxypropoxy)-3-methylphenyl)pentan-3-yl)-1-ethyl-N-neopentyl-1H-pyrrole-2-carboxamide (15b). By the same manner as described for the preparation of **13a**, compound **15b** was prepared from the intermediate **14b**. Yield: 58%.

N-(cyclopropylmethyl)-4-(3-(4-(2,3-dihydroxypropoxy)-3-methylphenyl)pentan-3-yl)-1-ethyl-1H-pyrrole-2-carboxamide (15c). By the same manner as described for the preparation of **13a**, compound **15c** was prepared from the intermediate **14c**. Yield: 47%.

4-(3-(4-(2,3-dihydroxypropoxy)-3-methylphenyl)pentan-3-yl)-1-ethyl-N-(2-hydroxyethyl)-1H-pyrrole-2-carboxamide (15d). By the same manner as described for the preparation of **13a**, compound **15d** was prepared from the intermediate **14d-OH**. Yield: 54%.

4-(3-(4-(2,3-dihydroxypropoxy)-3-methylphenyl)pentan-3-yl)-1-ethyl-N-(2,2,2-trifluoroethyl)-1H-pyrrole-2-carboxamide (15e). By the same manner as described for the preparation of **13a**, compound **15e** was prepared from the intermediate **14e**. Yield: 78%.

4-(3-(4-(2,3-dihydroxypropoxy)-3-methylphenyl)pentan-3-yl)-1-ethyl-N-(1-hydroxypropan-2-yl)-1H-pyrrole-2-carboxamide (15f). By the same manner as described for the preparation of **13a**, compound **15f** was prepared from the intermediate **14f-OH**. Yield: 72%.

4-(3-(4-(2,3-dihydroxypropoxy)-3-methylphenyl)pentan-3-yl)-1-ethyl-N-(1-hydroxy-3-methylbutan-2-yl)-1H-pyrrole-2-carboxamide (15g). By the same manner as

described for the preparation of **13a**, compound **15g** was prepared from the intermediate **14g-OH**. Yield: 66%.

4-(3-(4-(2,3-dihydroxypropoxy)-3-methylphenyl)pentan-3-yl)-1-ethyl-N-pentyl-1H-pyrrole-2-carboxamide (15h). By the same manner as described for the preparation of **13a**, compound **15h** was prepared from the intermediate **14h**. Yield: 76%.

4-(3-(4-(2,3-dihydroxypropoxy)-3-methylphenyl)pentan-3-yl)-1-ethyl-N-(3-hydroxypropyl)-1H-pyrrole-2-carboxamide (15i). By the same manner as described for the preparation of **13a**, compound **15i** was prepared from the intermediate **14i**. Yield: 69%.

Ethyl4-(4-(3-(1-ethyl-5-((2-hydroxy-2-methylpropyl)carbamoyl)-1H-pyrrol-3-yl)pentan-3-yl)-2-methylphenoxy)butanoate (16a). To a solution of the intermediate **14a** (386 mg, 1 mmol) in DMF, NaH (80 mg, 2 mmol) was added at portion-wise at 0 °C. The reaction mixture was stirred at 0 °C for 1 h and then added ethyl 4-bromobutyrate (291 mg, 1.5 mmol). The reaction mixture was moved to 25 °C for 5 h and then added H_2O (10 mL). The solution was extracted with ethyl acetate, and aqueous phase was extracted with ethyl acetate. The combined organic phases were washed with brine and then dried over anhydrous Na_2SO_4 and evaporated. The residue was purified by column chromatography (CH_2Cl_2/CH_3OH = 100/1) to give compound **16a** as white solid (290 mg, 58% yield).

Ethyl5-(4-(3-(1-ethyl-5-((2-hydroxy-2-methylpropyl)carbamoyl)-1H-pyrrol-3-yl)pentan-3-yl)-2-methylphenoxy)pentanoate (16b). By the same manner as described for the preparation of **16a**, compound **16b** was prepared from the intermediate **14a**. Yield:

67%.

4-(4-(3-(1-ethyl-5-((2-hydroxy-2-methylpropyl)carbamoyl)-1H-pyrrol-3-yl)pentan-3-yl)-2-methylphenoxy)butanoic acid (17a). To a solution of the intermediate **16a** (200 mg, 0.4 mmol) in ethanol, KOH (67 mg, 1.2 mmol) in H_2O was added and the reaction mixture was stirred at 80 °C for 5 h. The solution was diluted with H_2O (20 mL) and the pH value was adjusted to about 3-4 using 1 M HCl. Then it was extracted with ethyl acetate. The aqueous phase was extracted with ethyl acetate. The combined organic phases were washed with brine and then dried over anhydrous Na_2SO_4 and evaporated. The residue was purified by column chromatography with petroleum ether/ethyl acetate (10/1, v/v) to give the intermediate **17a** as yellow oil (180 mg, 95%).

5-(4-(3-(1-ethyl-5-((2-hydroxy-2-methylpropyl)carbamoyl)-1H-pyrrol-3-yl)pentan-3-yl)-2-methylphenoxy)pentanoic acid (17b). By the same manner as described for the preparation of **17a**, compound **17b** was prepared from the intermediate **16b**. Yield: 87%.

4-(3-(1-ethyl-5-((2-hydroxy-2-methylpropyl)carbamoyl)-1H-pyrrol-3-yl)pentan-3-yl)-2-methylphenyl (tert-butoxycarbonyl)alaninate (18a). To a solution of the intermediate **14a** (386 mg, 1 mmol) in CH_2Cl_2 (10 mL) was added Et_3N (418 μL, 3 mmol), followed by Boc-alanine (153 mg, 1.5 mmol), EDCI (288 mg, 1.5 mmol) and DMAP (12 mg, 0.1 mmol). The reaction mixture was stirred at 25 °C overnight and then poured into H_2O. The solution was extracted with CH_2Cl_2, and aqueous phase was extracted with CH_2Cl_2. The combined organic phases were washed with H_2O, brine, then

dried over anhydrous Na_2SO_4 and evaporated. The residue was purified by column chromatography with petroleumether/ethyl acetate (4/1, v/v) to give compound **18a** as white solid (197 mg, 43% yield).

4-(3-(1-ethyl-5-((2-hydroxy-2-methylpropyl)carbamoyl)-1H-pyrrol-3-yl)pentan-3-yl)-2-methylphenyl 3-((tert-butoxycarbonyl)amino)propanoate (18b). By the same manner as described for the preparation of **18a**, intermediate **18b** was prepared from the intermediate **14a**. Yield: 52%.

4-(3-(1-ethyl-5-((2-hydroxy-2-methylpropyl)carbamoyl)-1H-pyrrol-3-yl)pentan-3-yl)-2-methylphenyl alaninate (19a). To a solution of the intermediate **18a** (386 mg, 1 mmol) in CH_2Cl_2 (10 mL) was added TFA (2 mL) portion-wise. The reaction mixture was stirred at 0 °C for 2 h and then poured into H_2O. The solution was extracted with CH_2Cl_2, and aqueous phase was extracted with CH_2Cl_2. The combined organic phases were washed with H_2O, brine, then dried over anhydrous Na_2SO_4 and evaporated. The residue was purified by column chromatography with petroleum ether/ethyl acetate (4/1, v/v) to give compound **19a** as white solid (84 mg, 87% yield).

4-(3-(1-ethyl-5-((2-hydroxy-2-methylpropyl)carbamoyl)-1H-pyrrol-3-yl)pentan-3-yl)-2-methylphenyl 3-aminopropanoate (19b). By the same manner as described for the preparation of **19a**, compound **19b** was prepared from the intermediate **18b**. Yield: 92%.

4-(4-(3-(1-ethyl-5-((2-hydroxy-2-methylpropyl)carbamoyl)-1H-pyrrol-3-yl)pentan-3-yl)-2-methylphenoxy)-4-oxobutanoic acid (20). By the same manner as described for

the preparation of **16a**, compound **20** was prepared from the intermediate **14a**. Yield: 43%.

Molecule docking.

Molecular docking was performed with CDOCKER program that is interfaced with Discovery Studio 3.0. The crystal structure of VDR in complex with LG190178 (ID: 2ZFX) was obtained from protein data bank (PDB). All the water and ligands were removed and the random hydrogen atoms were added. The structures of the synthesized compounds were generated and minimized using tripos force fields. The highest-scored conformation based on the CDOCKER scoring functions, was selected as the final bioactive conformation.

VDR binding assay.

The assay was performed using a PolarScreen VDR Competitor Assay Red kit. The assay measures the decrease in mP accompanying loss of binding to the relatively high molecular weight VDR ligand binding domain of the fluorescent tracer due to the presence of a competitor. The compounds were supplied in a 10 mM DMSO solution, and VDR binding affinity was determined by Polar Screen™ VDR Competitor Assay. All compounds were tested for their binding affinity at 100 nM in triplicates. The affinity observed at 100 nM was used to set relative IC_{50} value. Fluorescence polarization was measured on an Ultra384microplate reader (Tecan) using a 535 nm excitation filter (25 nm bandwidth) and 590 nm emission filter (20 nm bandwidth). Finally, the relative IC_{50}

values of compounds were calculated using Graph Pad Prism 5.0.

Transcription assay.

Luciferase activity assay was performed using the Dual-Luciferase Reporter Assay System (Promega, Madison, WI) according to the manufacturer's instructions. HEK293 cells of 85%-90% confluence were seeded in 48-well plates. Transfections of 140 ng of TK-*SPP* × 3-*Luci* reporter plasmid, 20 ng of pCMX-*Renilla*, 30 ng of pENTER-CMV-*hRXRα* and 100 ng of pCMX-*VDR* for each well using Lipofectamine®2000 Reagent (Invitrogen). Eight hours after transfection, test compounds were added. Luciferase activity assay was performed 24 hours later using the Dual-Luciferase Assay System. Firefly luciferase activity was normalized to the corresponding Renilla luciferase activity. All the experiments were performed three times.

Anti-collagen I synthetic activity assay.

Anti-collagen I synthetic activity assay was performed using the human collagen I ELISA Kit (Elabscience, Wuhan). LX-2 cells obtained from American Type Culture Collection were maintained in Gibco 1640 medium supplement with 10% fetal bovine serum (FBS) and 1% Penicillin-Streotomycin. Approximate 1×10^5 cells, suspended in medium, were plated into each well of a 24-well plate and grown at 37°C in humidified atmosphere with 5% CO_2 for 24 h. The following day tested compounds at the concentration of 100 nM were added to the culture medium and incubated for 24 h.

Centrifuge supernate for 20 minutes to remove insoluble impurity and cell debris at 1000g at 2-8°C. Collect the clear supernate and carry out the assay immediately. Then follow the description of the Kit. Finally, the optical density (OD) is measured spectrophotometrically at a wavelength of 450 nm ± 2 nm. The OD value is proportional to the concentration of human collagen I.

Small interfering RNA (siRNA) transfection.

A VDR-directed siRNA and a scrambled siRNA were purchased from RIBOBIO Biotechnologies (Guangzhou, China). Transfection was carried out at a concentration of 50 nM using Lipofectamine®2000 Reagent (Invitrogen). Transfected cells were cultured 24 h prior to terminal assays.

The CCl_4-inducedmouse hepatic fibrosis model.

This study was carried out in strict accordance with the recommendations in the Guide for the Care and Use of Laboratory Animals of the National Institutes of Health. The protocol was approved by the Experimentation Ethics Review Committee of China Pharmaceutical University. All surgery was performed under sodium pentobarbital anesthesia, and all efforts were made to minimize suffering.

Male C57BL/6J mice (8 weeks old) were purchased from the Medical School of Yangzhou University (Yangzhou, China). All mice were maintained under standard conditions with free access to water and laboratory rodent food. To set up CCl_4-induced

mouse hepatic fibrosis model, mice were IP injected with 0.5 mL/kg bodyweight CCl_4 (1:50 v/v in corn oil from Sigma) three times a week for 4 weeks. Control mice received vehicle (DMSO in corn oil) instead. For the evaluation of the effect of Vitamin D Analogues on CCl_4-induced mouse hepatic fibrosis, 20 days after the first dose of CCl_4, calcipotriol, $1,25(OH)_2D_3$ or compound **15a** (20 μg/kg body weight) was administered by oral gavage five times a week. Mice were sacrificed 72 h after the final CCl_4 injection. Mouse livers and serum were obtained for histopathology, collagen assay, biochemical, and molecular analyses.

Lab data detection of serum sample.

Serum was collected from blood after centrifugation at 3000 rpm for 15 min at 4°C. Serum alanine amino transferase (ALT), aspartic transaminase (AST) and Total bile acid (TBA) were detected using commercial kits according to the manufacturer's instructions.

Histology.

Livers were fixed in 4% (w/v) neutral phosphate-buffered paraformaldehyde for 24 h, dehydrated, transparentized and embedded in paraffin. Liver tissues were cut into 5 μm sections which were stained with hematoxylin-eosin (H&E) for structured observation, or with Masson's trichrome stain for detection of collagen deposits. Determination of hydroxyproline content was carried out using a kit from Nanjing Jian Cheng Bioengineering Institute (Nanjing, China) according to the instruction by the manufacturer.

Immunohistochemistry analysis.

Immunohistochemistry staining for detection of HSC activation in vivo was performed as previously described. Briefly, the slides were gotten rid of paraffin, subjected to antigenretrieval, and quenching of endogenous peroxidase activity using 3% (v/v) H_2O_2 for 10 min. Immune complexes were visualized using suitable peroxidase-coupled secondary antibodies, according to the manufacturer's protocol (SP-9000 D 2-step plus poly-HR Panti-mouse/rabbit IgG detection system, ZSGB-BIO; Beijing, China). Mouse anti-α-SMA was employed as the primary antibody (Boster, Wuhan, China). The secondary antibodies incubated were horseradish peroxidase-conjugated goat anti-mouse IgG (Boster, Wuhan, China).

RNA extraction and quantitative real-time polymerasechain reaction (Q-PCR).

cDNA was generated from RNA extracts derived from cultured LX-2 cells and liver tissues using a reverse transcription kit (Transgen, Beijing, China). *β-actin* (mouse) or *U36B4* (human) was used as an internal control. Q-PCR was performed using the SYBR Green Master Mix (Vazyme). Primer pairs of mRNA used are as shown in Table S2.

Western blot.

Proteins were purified from LX-2 cells. Proteins were separated using 10% SDS-polyacrylamide gel electrophoresis and were electrophoretically transferred to polyvinylidene fluoride (PVDF) membranes using standard procedures. The following

primary antibodies were employed: mouse anti-α-SMA (Boster, Wuhan, China), rabbit anti-collagenI (Boster, Wuhan, China), muse anti-VDR (Santa Cruz, Inc), and mouse anti-β-actin (Boster, Wuhan, China). Horseradish peroxidase-conjugated goat anti-rabbit/mouse IgG (Boster, Wuhan, China) was used as the secondary antibody. Immunoreactive protein bands were detected using an Odyssey Scanning System (LI-COR Inc).

Pharmacokinetics Study.

Compounds **15a** and 1,25$(OH)_2D_3$ were dissolved in ethanol/EL/saline (1:1:18). Male Sprague-Dawley (SD) rats (n = 3) weighing 180-220 g were injected with these compounds intravenously (5 mg/kg) or intragastrically (20 mg/kg). Blood plasma samples were collected at 5, 15, 30 min and 1h, 2 h, 4 h, 8 h, 12 h, 24 h after administration of compounds, and then immediately centrifuged (12000 rpm, 10 min) to obtain plasma samples. The concentration of compounds in plasma was measured by HPLC. The pharmacokinetic parameters were calculated using Kinetica 4.4 software.

Statistical Analysis.

Data were expressed as means ± SD from at least three independent experiments. The differences between groups were analyzed for significance by t test when only two groups were compared or by one-way analysis of variance (ANOVA). All statistical analysis was performed using SPSS for windows version 11.0 (SPSS, Chicago, IL).

ASSOCIATED CONTENT

Supporting Information

List:

Table S1. The cytotoxicities of synthesized compounds against LX-2 cells.

Table S2. Primers used for PCR analysis.

Table S3. Pharmacokinetic Parameters of compounds **15a** and $1,25(OH)_2D_3$ in rats.

Figure S1. Relative expression of *CYP24A1* mRNA in LX-2 cells incubated with compound for 24 hours was measured by Q-PCR.

Figure S2. Relative expression of *Cyp24a1* mRNA in liver was measured by Q-PCR.

Figure S3. Relative expression of *Trpv6* mRNA in mouse intestine was measured by Q-PCR.

NMR spectra information

^{1}H NMR and ^{13}C NMR spectra of compounds

Molecular Formula Strings (CSV)

AUTHOR INFORMATION

Corresponding Author

Can Zhang*

*E-mail: zhangcan@cpu.edu.cn.

Author Contributions

The manuscript was written through contributions of all authors. All authors have given approval to the final version of the manuscript. [1]These authors contributed equally to this work.

Notes

The authors declare no competing financial interest.

ACKNOWLEDGMENT

The authors thank Public platform of State Key Laboratory of Natural Medicine and this work was supported by the National Natural Science Foundation of China (81273468, 81473153, 81703585), National Basic Research Program of China (2015CB755500), Fundamental Research Funds for the Central Universities of China (2632017PY10), 111 Project from the Ministry of Education of China and the State Administration of Foreign Expert Affairs of China (No. 111-2-07), the fund of Fujian Provincial Key Laboratory of Hepatic Drug Research (KFLX2018002), and the Open Project of State Key Laboratory of Natural Medicines (No. SKLNMZZCX201811).

ABBREVIATIONS USED

ALT, alanine transaminase; AST, aspartate transaminase; CCl_4, carbon tetrachloride; DRIPs, VDR interacting proteins; ECM, extracellular matrix; HSCs, hepatic stellate cells;

IP, intraperitoneal; LBP, ligand binding pocket; NAFLD, nonalcoholic fatty liver disease; NASH, nonalcoholic steatohepatitis; RNAi, RNA interference; SARs, structure-activity relationships; TBA, total bile acid; TGF, transforming growth factor; VDR, vitamin D receptor.

REFERENCES

(1) Bataller R, Brenner DA. Liver fibrosis. *The Journal of clinical investigation* **2005**, 115, 209-218.

(2) Hernandez-Gea V, Friedman SL. Pathogenesis of liver fibrosis. *Annual review of pathology* **2011**, 6, 425-456.

(3) Lee UE, Friedman SL. Mechanisms of hepatic fibrogenesis. *Best practice & research Clinical gastroenterology* **2011**, 25, 195-206.

(4) Friedman SL. Liver fibrosis -- from bench to bedside. *Journal of hepatology* **2003**, 38 Suppl 1, S38-53.

(5) Siegmund SV, Dooley S, Brenner DA. Molecular mechanisms of alcohol-induced hepatic fibrosis. *Digestive diseases* **2005**, 23, 264-274.

(6) Friedman SL, Bansal MB. Reversal of hepatic fibrosis -- fact or fantasy? *Hepatology* **2006**, 43, S82-88.

(7) Said A, Lucey MR. Liver transplantation: an update 2008. *Current opinion in gastroenterology* **2008**, 24, 339-345.

(8) Williams R. Global challenges in liver disease. *Hepatology* **2006**, 44, 521-526.

(9) Cohen-Naftaly M, Friedman SL. Current status of novel antifibrotic therapies in patients with chronic liver disease. *Therapeutic advances in gastroenterology* **2011**, 4, 391-417.

(10) Friedman SL. Hepatic stellate cells: protean, multifunctional, and enigmatic cells of the liver. *Physiological reviews* **2008**, 88, 125-172.

(11) Zhang DY, Friedman SL. Fibrosis-dependent mechanisms of hepatocarcinogenesis. *Hepatology* **2012**, 56, 769-775.

(12) Breitkopf K, Godoy P, Ciuclan L, Singer MV, Dooley S. TGF-beta/smad signaling in the injured liver. *Zeitschrift fur Gastroenterologie* **2006**, 44, 57-66.

(13) Inagaki Y, Okazaki I. Emerging insights into transforming growth factor beta smad signal in hepatic fibrogenesis. *Gut* **2007**, 56, 284-292.

(14) Cao H, Yu J, Xu W, Jia X, Yang J, Pan Q, Zhang Q, Sheng G, Li J, Pan X, Wang Y, Li L. Proteomic analysis of regenerating mouse liver following 50% partial hepatectomy. *Proteome science* **2009**, 7, 48.

(15) Abramovitch S, Dahan-Bachar L, Sharvit E, Weisman Y, Ben Tov A, Brazowski E, Reif S. Vitamin D inhibits proliferation and profibrotic marker expression in hepatic stellate cells and decreases thioacetamide-induced liver fibrosis in rats. *Gut* **2011**, 60, 1728-1737.

(16) Halder SK, Goodwin JS, Al-Hendy A. 1,25-Dihydroxyvitamin D3 reduces TGF-beta3-induced fibrosis-related gene expression in human uterine leiomyoma

cells. *The Journal of clinical endocrinology and metabolism* **2011**, 96, E754-762.

(17) Byers T. Anticancer vitamins du Jour--The ABCED's so far. *American journal of epidemiology* **2010**, 172, 1-3.

(18) Feldman D, Krishnan AV, Swami S, Giovannucci E, Feldman BJ. The role of vitamin D in reducing cancer risk and progression. *Nature reviews Cancer* **2014**, 14, 342-357.

(19) Gascon-Barre M, Demers C, Mirshahi A, Neron S, Zalzal S, Nanci A. The normal liver harbors the vitamin D nuclear receptor in nonparenchymal and biliary epithelial cells. *Hepatology* **2003**, 37, 1034-1042.

(20) Ding N, Yu RT, Subramaniam N, Sherman MH, Wilson C, Rao R, Leblanc M, Coulter S, He M, Scott C, Lau SL, Atkins AR, Barish GD, Gunton JE, Liddle C, Downes M, Evans RM. A vitamin D receptor/smad genomic circuit gates hepatic fibrotic response. *Cell* **2013**, 153, 601-613.

(21) Perakyla M, Malinen M, Herzig KH, Carlberg C. Gene regulatory potential of nonsteroidal vitamin D receptor ligands. *Molecular endocrinology* **2005**, 19, 2060-2073.

(22) Sato M, Lu J, Iturria S, Stayrook KR, Burris LL, Zeng QQ, Schmidt A, Barr RJ, Montrose-Rafizadeh C, Bryant HU, Ma YL. A nonsecosteroidal vitamin D receptor ligand with improved therapeutic window of bone efficacy over hypercalcemia. *Journal of bone and mineral research : the official journal of the American Society for Bone and Mineral Research* **2010**, 25, 1326-1336.

(23) Na S, Ma Y, Zhao J, Schmidt C, Zeng QQ, Chandrasekhar S, Chin WW, Nagpal S. A nonsecosteroidal vitamin d receptor modulator ameliorates experimental autoimmune encephalomyelitis without causing hypercalcemia. *Autoimmune diseases* **2011**, 2011, 132958.

(24) Plum LA, DeLuca HF. Vitamin D, disease and therapeutic opportunities. *Nature reviews Drug discovery* **2010**, 9, 941-955.

(25) Carlberg C, Molnar F. Current status of vitamin D signaling and its therapeutic applications. *Current topics in medicinal chemistry* **2012**, 12, 528-547.

(26) Belorusova AY, Rochel N. Modulators of vitamin D nuclear receptor: recent advances from structural studies. *Current topics in medicinal chemistry* **2014**, 14, 2368-2377.

(27) Yamada S, Makishima M. Structure-activity relationship of nonsecosteroidal vitamin D receptor modulators. *Trends in pharmacological sciences* **2014**, 35, 324-337.

(28) Makishima M. Current Topics on Vitamin D. Nonsecosteroidal vitamin D mudulators and prospects for their thepapeutic application. *Clinical calcium* **2015**, 25, 403-411.

(29) Boehm MF, Fitzgerald P, Zou A, Elgort MG, Bischoff ED, Mere L, Mais DE, Bissonnette RP, Heyman RA, Nadzan AM, Reichman M, Allegretto EA. Novel nonsecosteroidal vitamin D mimics exert VDR-modulating activities with less calcium mobilization than 1,25-dihydroxyvitamin D3. *Chemistry & biology* **1999**,

6, 265-275.

(30) Fujii S, Masuno H, Taoda Y, Kano A, Wongmayura A, Nakabayashi M, Ito N, Shimizu M, Kawachi E, Hirano T, Endo Y, Tanatani A, Kagechika H. Boron cluster-based development of potent nonsecosteroidal vitamin D receptor ligands: direct observation of hydrophobic interaction between protein surface and carborane. *Journal of the American Chemical Society* **2011**, 133, 20933-20941.

(31) Fujii S, Kano A, Masuno H, Songkram C, Kawachi E, Hirano T, Tanatani A, Kagechika H. Design and synthesis of tetraol derivatives of 1,12-dicarba-closo-dodecaborane as non-secosteroidal vitamin D analogs. *Bioorganic & medicinal chemistry letters* **2014**, 24, 4515-4519.

(32) Fujii S, Kano A, Songkram C, Masuno H, Taoda Y, Kawachi E, Hirano T, Tanatani A, Kagechika H. Synthesis and structure-activity relationship of p-carborane-based non-secosteroidal vitamin D analogs. *Bioorganic & medicinal chemistry* **2014**, 22, 1227-1235.

(33) Fujii S, Sekine R, Kano A, Masuno H, Songkram C, Kawachi E, Hirano T, Tanatani A, Kagechika H. Structural development of p-carborane-based potent non-secosteroidal vitamin D analogs. *Bioorganic & medicinal chemistry* **2014**, 22, 5891-5901.

(34) Shen W, Xue J, Zhao Z, Zhang C. Novel nonsecosteroidal VDR agonists with phenyl-pyrrolyl pentane skeleton. *Eur J Med Chem* **2013**, 69, 768-778.

(35) Ge Z, Hao M, Xu M, Su Z, Kang Z, Xue L, Zhang C. Novel nonsecosteroidal

VDR ligands with phenyl-pyrrolyl pentane skeleton for cancer therapy. *Eur J Med Chem* **2016**, 107, 48-62.

(36) Hao M, Hou S, Xue L, Yuan H, Zhu L, Wang C, Wang B, Tang C, Zhang C. Further developments of the phenyl-pyrrolyl pentane series of nonsteroidal vitamin d receptor modulators as anticancer agents. *Journal of medicinal chemistry* **2018**, 61, 3059-3075.

(37) Kudo T, Ishizawa M, Maekawa K, Nakabayashi M, Watarai Y, Uchida H, Tokiwa H, Ikura T, Ito N, Makishima M, Yamada S. Combination of triple bond and adamantane ring on the vitamin D side chain produced partial agonists for vitamin D receptor. *Journal of medicinal chemistry* **2014**, 57, 4073-4087.

(38) Liu C, Zhao GD, Mao X, Suenaga T, Fujishima T, Zhang CM, Liu ZP. Synthesis and biological evaluation of 1alpha,25-dihydroxyvitamin D3 analogues with aromatic side chains attached at C-17. *Eur J Med Chem* **2014**, 85, 569-575.

(39) Watarai Y, Ishizawa M, Ikura T, Zacconi FC, Uno S, Ito N, Mourino A, Tokiwa H, Makishima M, Yamada S. Synthesis, biological activities, and x-ray crystal structural analysis of 25-hydroxy-25(or 26)-adamantyl-17-[20(22),23-diynyl]-21-norvitamin D compounds. *Journal of medicinal chemistry* **2015**, 58, 9510-9521.

(40) Salem NA, Hamza A, Alnahdi H, Ayaz N. Biochemical and molecular mechanisms of platelet-rich plasma in ameliorating liver fibrosis induced by dimethylnitrosurea. *Cellular physiology and biochemistry : international journal*

of experimental cellular physiology, biochemistry, and pharmacology **2018**, 47, 2331-2339.

(41) Ma Y, Khalifa B, Yee YK, Lu J, Memezawa A, Savkur RS, Yamamoto Y, Chintalacharuvu SR, Yamaoka K, Stayrook KR, Bramlett KS, Zeng QQ, Chandrasekhar S, Yu XP, Linebarger JH, Iturria SJ, Burris TP, Kato S, Chin WW, Nagpal S. Identification and characterization of noncalcemic, tissue-selective, nonsecosteroidal vitamin D receptor modulators. *The Journal of clinical investigation* **2006**, 116, 892-904.

Lists of Captions:

Figure 1. Chemical structures of representative secosteroidal and nonsecosteroidal VDR ligands.

Figure 2. Design of the novel nonsecosteroidal VDR ligands.

Figure 3. Transcriptional activities of the compounds were examined. HEK293 cells were co-transfected with TK-*SPP* × 3-*Luci* reporter plasmid, pCMX-*Renilla*, pENTER-CMV-*hRXRα* and pCMX−*VDR*. Eight hours after transfection, test compounds, calcipotriol and 1,25$(OH)_2D_3$ were added. 24 hours later, luciferase activity assay was performed using the Dual-Luciferase Assay System. Renilla luciferase activity was as the reference to normalize the firefly luciferase activity. All the experiments were performed

three times. *P< 0.05 vs. DMSO.

Figure 4. Effects of compounds on activation of LX-2 cells. LX-2 cells were cultured with compounds, calcipotriol or 1,25$(OH)_2D_3$ for 24 hours at 100 nM. (A and B) The expression levels of *ACTA2* and *COL1A1* were measured by Q-PCR. (C and D) Expression of α-SMA and collagen I on LX-2 cells was determined by western blot. The representative gel electrophoresis bands are shown (C), and expression levels of proteins were normalized to the expression of β-actin (D). Densitometry data are shown as mean ± SD. *P< 0.05 vs. TGFβ1, $^{\#}P$< 0.05 vs. TGFβ1+Calcipotriol.

Figure 5. 15a inhibited activation of LX-2 cells via VDR. (A) *VDR*-specific (siVDR) or negative control (siNC) siRNA-transfected LX-2 cells were treated with **15a** (100 nM), TGFβ1 (1 ng/mL), or TGFβ1 plus **15a** for 24 hours. The expression of VDR, α-SMA and collagen I on LX-2 cells was tested by western blot. The representative gel electrophoresis bands are shown. (B, C and D) Expression levels of VDR, collagen I and α-SMA were normalized to the expression of β-actin. The quantified densitometry data are shown as mean ± SD. *P< 0.05.

Figure 6. **15a** suppressed the expression of α-SMA in CCl_4-induced hepatic fibrosis lesions and protected the liver from impairment. Mice (n=5 in each group) received either DMSO or CCl_4 (0.5 mL/kg body weight) intraperitoneally for three weeks before intragastric administration of **15a**, calcipotriol, 1,25$(OH)_2D_3$ (20 μg/kg body weight) or DMSO. (A) α-SMA expression in the injured liver was tested by immunohistochemistry

(×200). (B) The expression levels of α-SMA were quantified using Image-Pro Plus 6.0. Data are shown as mean ± SD. $^{*}P < 0.05$ vs. CCl_4. (C) Expression of *Acta2* in the injured liver was examined by Q-PCR (mean ± SD. $^{*}P < 0.05$).

Figure 7. **15a** inhibited the CCl_4-induced hepatic lesions and collagen deposition. Mice (n=5 in each group) received either DMSO or CCl_4 (0.5 mL/kg body weight) intraperitoneally for three weeks before intragastric administration of **15a**, calcipotriol, $1,25(OH)_2D_3$ (20 μg/kg body weight) or DMSO. (A) CCl_4-induced hepatic fibrosis lesions were examined by H&E staining (×100), the collagen deposition was determined by Masson's trichrome staining (×200) and hydroxyl proline measurement (mean ± SD. $^{*}P < 0.05$ vs. CCl_4) (A and B). (C) Expression of *Col1a1* in the injured liver was examined by Q-PCR (mean ± SD. $^{*}P < 0.05$).

Figure 8. **15a** protected the liver from impairment. Mice (n=5 in each group) received either DMSO or CCl_4 (0.5 mL/kg body weight) intraperitoneally for three weeks before intragastric administration of **15a**, calcipotriol, $1,25(OH)_2D_3$ (20 μg/kg body weight) or DMSO. (A, B, and C) The serum levels of ALT, AST and TBA were determined. (D) The serum calcium concentration was determined by calcium assay kit (mean ± SD. $^{*}P < 0.05$, $^{**}P < 0.01$).

Figure 9. (A) Superposition of compounds **15a** and $1,25(OH)_2D_3$. Compound **15a** is depicted in green and $1,25(OH)_2D_3$ is depicted in red. (B) Superposition of compounds **15a** and YR301. **15a** is depicted in green and YR301 is in pink. (C) Docking structure of

the complex **15a**-VDR. The ligands are exhibited in stick representation, carbon is depicted in cyan and oxygen atoms in red. The hydrogen bonds that formed between ligands and VDR are exhibited as yellow dashed lines.

Scheme 1. Synthesis of compounds **13a-h**[a]

Scheme 2. Synthesis of compounds **15a-i**[a]

Scheme 3. Synthesis of compounds **17a-b**, **19a-b**, and **20**[a]

Table 1. The structures of all compounds.

Table 2. The affinities of VDR binding and activities of anti-collagen I synthetic at 100 nM.

Highlights

1. Twenty-two novel compounds have been designed and synthesized.
2. Seven compounds have much higher potencies against the synthesis of collagen I *in vitro* than calcipotriol.
3. **15a** exhibited more efficient inhibitory activity against both collagen deposition and fibrotic gene expression in the western blot and Q-PCR assays.
4. **15a** treatment prevented hepatic fibrosis induced by CCl_4 injections in mice.
5. **15a** can not only display better results for the reduction of liver damage than

calcipotriol and 1,25$(OH)_2D_3$, but also had no significant change on serum calcium.

Table of Contents Graphic.

Good VDR agonistic activity

Significantly decreased the synthesis of collogen 1 *in vitro*

Marketly prevention in the progress of liver fibrosis

Improvements in liver function